

DISSERTATION

EXAMINATION OF THE POTENTIAL IMPACTS OF DUST AND POLLUTION AEROSOL
ACTING AS CLOUD NUCLEATING AEROSOL ON WATER RESOURCES IN THE
COLORADO RIVER BASIN

Submitted by

Vandana Jha

Department of Atmospheric Science

In partial fulfillment of the requirements

For the Degree of Doctor of Philosophy

Colorado State University

Fort Collins, Colorado

Spring 2016

Doctoral Committee:

Advisor: William R. Cotton

Steven A. Rutledge

Jeffery Pierce

Jorge Ramirez

Copyright by Vandana Jha 2016

All Rights Reserved

ABSTRACT

EXAMINATION OF THE POTENTIAL IMPACTS OF DUST AND POLLUTION AEROSOL ACTING AS CLOUD NUCLEATING AEROSOL ON WATER RESOURCES IN THE COLORADO RIVER BASIN

In this study we examine the cumulative effect of dust acting as cloud nucleating aerosol (cloud condensation nuclei (CCN), giant cloud condensation nuclei (GCCN), and ice nuclei (IN)) along with anthropogenic aerosol pollution acting primarily as CCN, over the entire Colorado Rocky Mountains from the months of October to April in the year 2004-2005; the snow year. This ~6.5 months analysis provides a range of snowfall totals and variability in dust and anthropogenic aerosol pollution. The specific objectives of this research is to quantify the impacts of both dust and pollution aerosols on wintertime precipitation in the Colorado Mountains using the Regional Atmospheric Modeling System (RAMS). In general, dust enhances precipitation primarily by acting as IN, while aerosol pollution reduces water resources in the CRB via the so-called “spill-over” effect, by enhancing cloud droplet concentrations and reducing riming rates. Dust is more episodic and aerosol pollution is more pervasive throughout the winter season. Combined response to dust and aerosol pollution is a net reduction of water resources in the CRB. The question is by how much are those water resources affected? Our best estimate is that total winter-season precipitation loss for the CRB the 2004-2005 winter season due to the combined influence of aerosol pollution and dust is 5,380,00 acre-feet of water. Sensitivity studies for different cases have also been run for the specific cases in 2004-2005 winter season to analyze the impact of changing dust and aerosol ratios on precipitation in the

Colorado River Basin. The dust is varied from 3 to 10 times in the experiments and the response is found to be non monotonic and depends on various environmental factors. The sensitivity studies show that adding dust in a wet system increases precipitation when IN affects are dominant. For a relatively dry system high concentrations of dust can result in over-seeding the clouds and reductions in precipitation. However, when adding dust to a system with warmer cloud bases, the response is non-monotonical, and when CCN affects are dominant, reductions in precipitation are found.

Keywords: Dust, Aerosol, CCN, GCCN, IN.

ACKNOWLEDGEMENTS

I would like to acknowledge my dissertation advisor, Dr. William Cotton, who is a great scientist and a greater human being. I feel lucky to have him as my mentor. I would also like to thank Dr. Steve Rutledge for being very encouraging and supporting me in my journey at CSU. I want to thank Dr. Jeffrey Pierce for the GEOS-Chem data and Dr. Jorge Ramirez for being on my committee. I want to thank Ted Letcher for getting me started with RAMS modeling in my first semester. I want to thank Steve Saleeby for the useful discussions regarding the Snotel and seasonal study. I would also like to thank the NSF for providing funding for my research. A special acknowledgement is extended to Dr. Gustavo Carriò for doing major contributions to the RAMS code and guiding me everyday during all these years.

I want to thank my parents for always supporting me in life. I want to thank my brother for doing the pep talk for joining the PhD in this department. I also want to thank all my friends for always being there by my side and believing in me. At last, I want to thank my canine friends Jane Brady and Betta for loving me selflessly.

This work was supported by the National Science Foundation Division of Atmospheric Sciences grant AGS 1138896 and I am grateful to NSF for this opportunity.

DEDICATION

~ I would like to dedicate this work to my maternal grandfather (my beloved Nana) who always motivated me to get a Ph.D. I hope he is watching me get this for real.

TABLE OF CONTENTS

ABSTRACT.....	ii
ACKNOWLEDGEMENTS.....	iv
DEDICATION.....	v
TABLE OF CONTENTS.....	vi
LIST OF TABLES	ix
LIST OF FIGURES	x
CHAPTER 1: Introduction.....	1
CHAPTER 2: A study on the impact of dust and aerosol pollution on precipitation in the Colorado River Basin: Part I - Seasonal Precipitation Estimates.....	4
2.1.0 Introduction.....	4
2.2.0 Background Research.....	7
2.3.0 Dust Impact on Microphysics.....	8
2.3.1 RAMS dust model.....	9
2.3.2 RAMS cloud microphysics.....	10
2.3.3.1 Setup 1 (old code)	10
2.3.3.2 Setup 2 (updated code)	11
2.3.3.2 Setup 3.....	11
2.3.4 The adsorption theory.....	12
2.3.5 New look-up table.....	13
2.3.6 Ice activation.....	15
2.3.7 The new ice nucleation scheme.....	15

2.3.8 Dust activation as GCCN.....	17
2.3.9 Precipitation scavenging.....	18
2.4.0 RAMS dynamic model setup.....	19
2.4.1 GEOS-Chem.....	21
2.5.0 Model Results.....	25
2.6.0 Conclusions.....	30
2.7.0 Discussion.....	31
2.8.1 Snotel observation and comparisons	33
2.8.2 Summary	36
2.9.0 References.....	39
CHAPTER 3: A study on the impact of dust and aerosol pollution on wintertime orographic precipitation in the Colorado River Basin: Part II Sensitivity Studies.....	43
3.1.0 Introduction.....	43
3.2.0 Summary of Part I	43
3.2.1 Methods.....	43
3.2.2 Experimental Methodology.....	44
3.3.0 Results and discussion.....	45
3.3.1: Case Study 1.....	45
3.3.2: Case Study 2	46
3.3.3: Case Study 3.....	57
3.4.0 Conclusion.....	64
3.5.0 References.....	65

CHAPTER 4: Summary and Future work	71
4.1.1 Overall Summary.....	71
4.2.1 Future Work.....	72
References	74
Appendix	75

LIST OF TABLES

Table 2.1: RAMS model configuration.....	21
Table 2.2: Comparison of integrals precipitation per period for setup 1.....	26
Table 3.1: Sensitivity Tests Types.....	44
Table 3.2: Results of dust sensitivities in the three Case Studies.....	64
Table A.1: Table for the basin wise difference in precipitation in the CRB.....	75

LIST OF FIGURES

Figure 2.1: The Colorado River Basin.....	5
Figure 2.2: Feeder-seeder cloud, adapted to the ice phase from storm and cloud dynamics by Cotton et al., (2010) (originally from Bergeron, 1965).....	8
Figure 2.3: CCN activation curves of different types.....	13
Figure 2.4: Comparison of ice nucleation parameterization with $cf = 3$ with the D10 parameterization for calculations in the mixed-phase cloud regime.....	17
Figure 2.5: The 3 grid configuration.....	19
Figure 2.6: Topography of the region shown in contour for Grid 1.....	21
Figure 2.7: Concentration of anthropogenic aerosol for the entire season.....	24
Figure 2.8: Concentration of anthropogenic dust for the entire season.....	24
Figure 2.9: CCN concentration for period 1.....	27
Figure 2.10: Dust concentration for period 1.....	27
Figure 2.11: CCN concentration for period 8.....	27
Figure 2.12: Dust concentration for period 8.....	27
Figure 2.13: Cloud diameter before the CCN peak for period 8.....	27
Figure 2.14: Cloud diameter after the CCN peak for period 8.....	27
Figure 2.15: CCN concentration for period 19.....	28
Figure 2.16: Dust concentration for period 19.....	28
Figure 2.17: CCN concentration for period 20.....	28
Figure 2.18: Dust concentration for period 20.....	28
Figure 2.19: Map for the regions for different river basin.....	28

Figure 2.20: Map for precipitation difference in both regions for different river basins in % for Period 1.....	29
Figure 2.21: Map for Precipitation difference in both regions for different river basin in % for the entire season.....	29
Figure 2.22: Integral mass of precipitation difference in both regions setup 1.....	29
Figure 2.23: Map for precipitation difference in both regions using setup 2.....	31
Figure 2.24: Map for precipitation difference in both regions for different river basins using the setup 2.....	31
Figure 2.25: Top: Total accumulated precipitation for the grid 3. Bottom: total accumulated precipitation difference in inches for Setup 2.....	32
Figure 2.26: Composite 500-hPa geopotential height (m) from the NARR dataset for 1 Oct- Apr 2005.....	34
Figure 2.27: Composite 500-hPa geopotential height anomaly from the NARR dataset for 1 Oct- Apr 2005.....	34
Figure 2.28: 700-hPa RH anomaly (%) from the NARR dataset for 1 Oct- Apr 2005.....	35
Figure 2.29: Total accumulated Comparison of RAMS precipitation with Snotel sites.....	35
Figure 2.30: Total accumulated Comparison of RAMS precipitation with Snotel sites.....	36
Figure 3.1a: Dust concentration profile for a1d1 for Case Study 1.....	47
Figure 3.1b: Dust concentration profile for a1d3 for Case Study 1.....	47
Figure 3.1c: Dust concentration profile for a1d10 for Case Study 1.....	48
Figure 3.2: Plot of precipitation with no dust compared to a1d3, a1d10, a1dccn, a1din.....	48
Figure 3.3: Plot of aggregates for the different cases.....	49
Figure 3.4: Temperature profile of study for the Case Study 1.....	49

Figure 3.5: Total precipitable water for grid 3 for the Case Study 1.....	50
Figure 3.6: 500 mb geopotential heights for the Case Study 1.....	50
Figure 3.7: Topography of Grid 3 of the area of study for the Case Studies.....	51
Figure 3.8: Plot for comparison of Snotel and RAMS snow water equivalent in inches.....	51
Figure 3.9a: Dust concentration profile for a1d1 for Case Study 2.....	52
Figure 3.9b: Dust concentration profile for a1d3 for Case Study 2.....	53
Figure 3.9c: Dust concentration profile for a1d10 for Case Study 2.....	53
Figure 3.10: CCN concentration profile for Case Study 2.....	54
Figure 3.11: Plot of precipitation with no dust compared to a1d1, a1d3, a1d10.....	54
Figure 3.12: Plot of precipitation with no dust compared to a1dcn and a1din.....	55
Figure 3.13: Temperature profile of study for the Case Study 2.....	55
Figure 3.14: Total precipitable water for grid 3 for the Case Study 2.....	56
Figure 3.15: 500 mb zonal wind speed for the Case Study 2.....	56
Figure 3.16: 500-hPa geopotential height (m) from the NARR dataset for Case Study 2.....	57
Figure 3.17: Dust concentration profile for a1d1 for Case Study.....	58
Figure 3.18: CCN concentration profile for the period for Case Study 3.....	58
Figure 3.19: Plot of cloud base temperature for the three case studies. Case Study 3 is dominated by lower cloud bases and hence higher cloud base temperatures.....	59
Figure 3.20: Plot of precipitation with no dust compared to a1d1 a1d3 a1d10 a1din.....	60
Figure 3.21: Comparison Total mass of water in drizzle category white: a1d1, green: a1d3 and red: a1d10.....	60
Figure 3.22: Total precipitable water for grid 3 for the Case Study 3.....	61

Figure 3.23: 500-hPa geopotential height (m) from the NARR dataset for Case Study 3.....61

Figure 3.24: Plot of precipitation with no dust compared to a1d1, a1d3, a1d10, a1din62

Figure 3.25: Plot of aerosol concentrations for the three case studies. Case Study 3 is the one that has higher concentration of aerosols.....62

Figure 3.26: Plot of precipitation for a) a1d1 b) a1d0 c) nant d) a1d3 e) a1d10.....63

CHAPTER 1

Introduction

The major consumer of water resources in the Colorado River Basin is agriculture as the river irrigates some 3.5 million acres of crops. Except for Arizona and Wyoming, agriculture dominates the consumption of the Colorado River Basin water resources. In fact, California's agriculture water consumption exceeds the total annual water consumption in any one of the other 7-member states.

Unfortunately, the southwest US experiences huge swings in precipitation largely due to natural causes associated with the El Nino Southern Oscillation (ENSO), multi-decadal variability of the North Atlantic and Pacific Oceans, as reflected by the Pacific Decadal Oscillation (PDO) and the Atlantic Multidecadal Oscillation (AMO). Superimposed on this large natural variability signal are climate forcings associated with human activity such as greenhouse gas forcings, land-use changes (which can contribute to dust production), and aerosol pollution. Against this background of large natural variability of annual precipitation in the southwest US, it is difficult to identify the contributions of human activity to annual precipitation variability purely through measurements. Models that can represent these forcings are needed to clearly identify causality of the observed changes in seasonal precipitation in the region.

The emphasis in this research is on the attribution of human activity to water resources in the CRB. While there have been recent attempts to quantify projected forcings by anthropogenic greenhouse gas emissions (McCabe and Wolock, 2007; Christensen et al., 2004; Christensen and Lettenmaier, 2007) on CRB water resources, there has been few attempts to quantify impacts of

aerosol pollution and dust on water resources in the CRB. The impacts of aerosol pollution and land-use changes, especially with dust production, on water resources in the CRB has been examined.

The goals and research outlined above is organized in this dissertation as follows. Chapter 2 examines the cumulative effect of dust acting as cloud nucleating aerosol (cloud condensation nuclei (CCN), giant cloud condensation nuclei (GCCN), and ice nuclei (IN)) along with anthropogenic aerosol pollution acting primarily as CCN, over the entire Colorado Rocky Mountains from the months of October to April in the year 2004-2005; the snow year. This ~6.5 months analysis provides a range of snowfall totals and variability in dust and anthropogenic aerosol pollution. The specific objectives of this research is to quantify the impacts of both dust and pollution aerosols on wintertime precipitation in the Colorado Mountains using the Regional Atmospheric Modeling System (RAMS). In Section 2.0 we discuss the previous relevant research as a means of placing the current study in scientific context. In section 2.3.0 the impact of dust and aerosol pollution on cloud microphysics has been discussed. The difference between the old and the new RAMS code has further been discussed. The methods for dust activation as IN in the code is described and how dust acting as GCCN works in RAMS, as well as how precipitation scavenging is dealt with. In Section 2.4.0 the model setup as well as the initial conditions and the experimental design in the current version of RAMS has been described. In Section 2.3.4 Kohler theory and its limitations when applied to dust and the corresponding advantages of using the adsorption theory for dust activation scheme has been discussed. The DeMott et al 2014 scheme of ice nucleation has been discussed in Section 2.3.7. In Section 2.4.1 the GEOS-Chem model for the generation of dust and various species of aerosol pollution is described. An overview of the model results is given

in Section 2.5.0 for the period of the winter-season simulations. A discussion is given in Section 2.6.0 between the results using the old code using Lerach (2012) CCN activation scheme using Kohler theory, and DeMott et al., 2012 IN scheme, and the new code using adsorption theory in the new look up table and the DeMott, 2014 IN scheme.

Chapter 3 has a description of the sensitivity studies and their impacts on different kinds of orographic cloud systems depending on different synoptic forcings and availability of moisture. Chapter 3 starts with an introduction of the orographic precipitation. The new RAMS droplet activation code is applied in sensitivity studies of a mixed-phase orographic cloud in northwestern Colorado. The sensitivity studies are 5 different kinds. The base study has both the dust and aerosol pollution data ON. The Case 2 has dust OFF with only the aerosol sources ON. The Case 3 has the aerosol sources ON with dust multiplied by a factor of 3. Case 4 has the aerosol sources ON with dust multiplied by a factor of 10. Case 5 and Case 6 are the simulations where dust can act only as CCN and only as IN respectively. It was found that the response is largely dependent on the environmental conditions and cloud base height and temperature of each experiment. For the colder cloud base regime in Case Study 1, the precipitation increases when dust is increased 3 times and ten times and IN effect dominates the system. However, in the Case Study 3, which has lower cloud base heights and the temperatures are warmer, the response of increasing dust 10 times is non-monotonic and the response also depends on the environmental conditions. Dust acting as CCN acts in opposition to dust acting as IN. In general, dust acting as IN tends to enhance precipitation in wintertime orographic clouds.

Finally, in Chapter 4 conclusions are offered with a focus on the implications for future studies and suggestions for their direction.

CHAPTER 2

A study on the impact of dust and aerosol pollution on precipitation in the Colorado River Basin: Part I - Seasonal Precipitation Estimates

2.1.0 Introduction

The southwest United States is a region with huge demands on water resources. The Colorado River Basin (CRB) covers the states of Colorado, Wyoming, Utah, Nevada, Arizona, New Mexico, and California as well as Mexico (Figure 2.1). The headwaters lie in the Rocky Mountains of Colorado and Wyoming. But the water resources in the CRB are potentially impacted by aerosol pollution and dust acting as cloud nucleating aerosol as well as dust affecting the albedo of the snowpack.

Saleeby et al. (2009) examined the hypothesis that high aerosol pollution acting as cloud concentration nuclei (CCN) leads to the formation of smaller, more numerous droplets and reduced riming. They also found that with higher CCN concentrations the smaller droplets evaporate more readily when ice crystals grow at the expense of cloud droplets (the Wegener-Bergeron-Findeisen process; WBF) depleting liquid water contents, but enhances ice particle vapor deposition growth. Thus overall precipitation was reduced only by a small amount owing to the compensating effects of the enhanced WBF process. Consistent with the Bory's hypothesis (Bory's et al., 2000), they found that reduced riming lowered snow water equivalent precipitation amounts on the windward side of the mountain barrier and increased it on the lee slopes. In the case of the Park Range, the "spillover effect" led to a downstream shift of precipitation from the Pacific watershed to the Atlantic watershed further contributing to a reduction of precipitation in the CRB. They also showed that this

effect was only important for relatively wet storms where riming is important. Storms producing clouds with low supercooled liquid water content (SLWC) are less influenced by aerosol pollution. These results are further supported by more recent studies, wherein Saleeby et al. (2011) estimated the total change in precipitation for all of western Colorado due to



Figure 2.1: The Colorado River Basin (source: <http://www.usbr.gov/lc/region/programs/crbstudy.html>)

aerosol pollution for a 60-day period for four different seasons. These simulations were performed for assumed high and low values of aerosol acting as CCN. Again, little change in total precipitation was found but a major shift in precipitation downwind, or spillover effect, was simulated owing to aerosol pollution. In that study the biggest loser was the CRB with as much as 522,000 acre-ft lost in a 60-day period in 2005.

Dust can also affect precipitation processes. Dust is known to act as a good ice nuclei (IN) (Schaefer, 1949, 1954; Isono et al., 1959; Roberts and Hallett, 1968; Zuberi et al., 2002; Hung et al., 2003; Gagin, 1965; Levi and Rosenfeld, 1996; Sassen et al., 2003; DeMott et al., 2003; 2009). Considering that the basis behind cloud seeding is to enhance precipitation by enhancing IN concentrations (Cotton and Pielke, 2007), we anticipate that dust serving as IN will enhance precipitation in wintertime orographic clouds. But if the dust becomes coated with sulfates or originates over dry lake beds, dust can serve as giant cloud condensation nuclei (GCCN) which when wetted can result in larger cloud droplets and thereby enhance the warm-cloud collision and coalescence process and ice particle riming. Dust serving as GCCN should enhance precipitation (Levin et al., 1996), thus acting to support the activity of IN. However, the major impact of GCCN is on enhancing the warm-rain collision and coalescence process, a process that is not very active in wintertime orographic clouds in Colorado. But smaller dust particles coated with sulfates can enhance droplet concentrations, leading to numerous smaller droplets and decreasing collision and coalescence of droplets and ice particle riming. Thus dust functioning as CCN will work in opposition to its activity as GCCN and IN and suppress precipitation much like pollution aerosol. In their study of the effects of African dust on deep convective precipitation over South Florida, van den Heever et al. (2006), found that dust serving as CCN had a stronger impact on precipitation than dust serving as GCCN or IN. No one to our knowledge has examined the combined effects of dust serving as IN, GCCN, and CCN on precipitation or on water resources in the CRB. Therefore, the focus of this study is on the impacts of dust and aerosol pollution acting as cloud nucleating aerosol on wintertime orographic precipitation in the Colorado Mountains. In Chapter 3 (Part II)

sensitivity studies for different cases have been run in the 2004 - 2005 winter season to analyze the impact of changing dust and aerosol ratios on precipitation in the Colorado River Basin.

2.2.0 Background Research

In an orographic ‘seeder-feeder’ cloud system (Figure 2.2), the orographic feeder cloud is formed by the forced ascent of flow over the hill. The formation of the orographic seeder cloud, which lies above the feeder cloud, is often due to large-scale ascent. The seeder cloud forms precipitation in the form of steady stratiform snowfall (or rainfall in warmer clouds) of light to moderate intensity, which would result in light surface snowfall in the absence of the orographic cloud. If the seeder cloud snowfall encounters the water-rich environment of the feeder cloud, the precipitation elements collect cloud droplets, thereby enhancing the snowfall (Cotton et al., 2010). An increase in CCN can lead to smaller/more numerous cloud droplets within the supercooled cloud region of an orographic ‘seeder-feeder’ cloud system (Borys et al., 2000). Smaller cloud droplets within the supercooled ‘feeder’ rime less efficiently onto pristine ice crystals that precipitate from the seeder cloud. This process affects the orographic snowfall in two different ways. First, it can delay or inhibit the conversion of cloud water into precipitation, and therefore, reduce the total amount of snowfall from the orographic storm. Secondly, the unrimed snowflakes can be advected downstream to the lee of the mountain into a subsiding region where ice crystals are likely to evaporate. Moreover, this downward shift is capable of changing the distribution of water resources in various water basins within these mountainous regions.

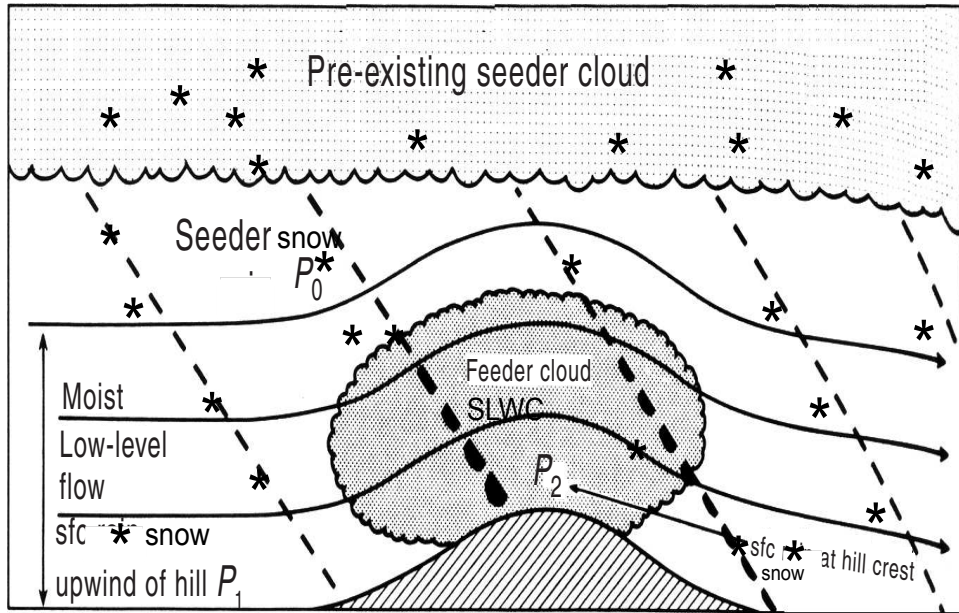


Figure 2.2: Feeder-seeder cloud, adapted to the ice phase from storm and cloud dynamics by Cotton et al., (2010) (originally from Bergeron, 1965).

2.3.0 Dust Impact on Microphysics

Whilst anthropogenic sources of aerosol particles are changing with human population and technology, natural sources are also impacted. Dust is a relatively large, globally transported natural aerosol source whose production is impacted by the changes to regional climate, especially the hydrologic cycle (Rosenfeld et al., 2001). Aerosol particles have also been identified to act on cloud microphysics, through the first and second indirect effects (Twomey, 1974; 1977; Albrecht, 1989). Dust aerosol particles have been shown to serve as both cloud condensation nuclei (CCN) (including giant, GCCN) and ice nuclei (IN) (DeMott et al., 2003; Twohy et al., 2005, 2009). Therefore, the presence of dust can possibly alter the formation of warm and mixed-phase clouds on the global scale due to the radiative (direct) and the microphysical (indirect) forcings.

2.3.1 RAMS dust model

The dust source and transport module incorporated into RAMS for this study (implemented by Smith, 2007 and revised by Lerach, 2010) is based on that of Ginoux et al. (2001), which advects lofted dust in two size bins: accumulation mode and coarse mode. The fine mode dust median radius was set to $0.2\mu\text{m}$, and the coarse mode dust median radius was set to $3.0\mu\text{m}$. These values were derived from limited AEROSOL ROBOTIC NETWORK (AERONET) observations at Sevilleta, NM (-106.885° , 34.35°) from 15 April 2003 at 2200 UTC. The dust simulation in RAMS is dependent on soil moisture, soil composition, wind speed, vegetative cover and composition (Prospero, 1999). A dust source function S , created by Ginoux et al. (2001) represents the fraction of dust produced by wind erosion. This source function is based on the work of Prospero (1999) relating the major global sources of dust with regional topographic depressions, as these areas can accumulate fine-particle sediments that are suitable for wind erosion and transport. Tegen and Fung (1994) characterize the soil mass fractions and size classes. Soil is divided into two broad classes: silt and clay. Silt is assumed to constitute the majority of erodible materials.

Silt is evenly partitioned into three size classes and is assigned 90% of all mass available for lofting. The remaining 10% is assumed to be clay in the sub-micron range, partitioned evenly into four size classes. The algorithm in RAMS follows the methods of Marticorena and Bergametti (2005), and hence parameterizes a threshold friction velocity, based on intrinsic particle characteristics as well as the roughness length of the surface. Mass emissions are dependent on the wind speed at 10 m, which is interpolated from the lowest model layer wind speed by assuming a logarithmic wind profile. The mass flux is converted to a number concentration assuming a density of 2500 kg m^{-3} for clay and 2650 kg m^{-3} for silt. The RAMS

dry deposition scheme is based on that of Wang et al. (2006) but modified for use with mineral dust.

2.3.2 RAMS cloud microphysics

The RAMS bin-emulating, two-moment bulk microphysics scheme (Feingold et al., 1998; Cotton et al., 2003; Saleeby and Cotton, 2004; 2008) is used in these simulations, in which the cloud droplet size distribution is decomposed into small cloud droplets (cloud1) and large cloud droplets (cloud2) (Saleeby and Cotton, 2004). The scheme explicitly predicts mixing ratios and number concentrations of pristine ice, snow, aggregates, graupel, hail, cloud1 and cloud2 droplets, and rain. Droplet collection, condensation, and evaporation are explicitly represented in this scheme. Two different schemes are used for droplet activation in this study.

2.3.3.1 Setup 1 (old code)

In the first approach, nucleation by CCN, GCCN, and IN is explicitly considered (Saleeby and Cotton, 2004; Ward et al., 2010). Lerach (2012) implemented a new lookup table in RAMS using a Lagrangian parcel model (Heymsfield and Sabin, 1989) in conjunction with the existing lookup table (Saleeby and Cotton, 2004). Dust is assigned a constant κ value of 0.03 (Petters et al., 2007) based on Koehler et al. (2009), for the Arizona test dust. The background median radius is held constant at 0.035 μm , while the background value of κ was set to 0.2. The lookup table activates potential CCN as a function of ambient vertical velocity, temperature, dust and background aerosol number concentrations, background aerosol κ parameter, and the median radii of the dust and background aerosol distributions. A Lagrangian parcel model (Heymsfield and Sabin, 1989) based relationship was created which parameterizes

the dust-GCCN activation as a function of predicted coarse mode, dust number concentration and ambient vertical velocity. Dust activation is based on Koehler theory.

2.3.3.2 Setup 2 (updated code)

The Setup 2 look-up table is designed to simulate the competitive interaction of three externally aerosol species; dust, sea spray salt, and ordinary natural soluble aerosol or pollution aerosol. For dust, which is large and largely insoluble, Koehler theory is replaced by an adsorption theory treatment (Kumar et al., 2011). For given environmental conditions, water adsorption effects on the insoluble dust particles can produce important reductions in the critical size and therefore significantly affect competition. In order to interface the RAMS droplet activation look-up tables with GEOS-Chem for pollution or clean background (no anthropogenic sources) aerosols, the concentration, and chemistry (via kappa) is derived by concentration weighting of three internally mixed groups of aerosols predicted by GEOS-Chem (inorganics, hydrophilic organics, and hydrophobic organics). The kappa and aerosol concentrations so-weighted, are then introduced locally to predict the concentration of those potential CCN that are activated to form cloud droplets. Adsorption theory is described in detail in the section 2.3.4.

2.3.3.3 Setup 3

Setup 3, is exactly the same as Setup 2 except now we consider dust sources to be present in the non-anthropogenic control run. This is done because, while anthropogenic sources of dust occur, they tend to be less than non-anthropogenic sources (Huang et al., 2015). Thus, the model was run for the same period (6.5 months) starting on October 1st and ending on April 20th. In this set of runs, the non-anthropogenic aerosol was turned ON. The local dust sources were turned ON from RAMS dust model as well as the dust from the GEOS-Chem was also turned ON and nudged into the RAMS. This was for the representation of both coarse (local dust sources) and

the fine mode dust particles (long range transport). The clean background or non-anthropogenic sources of aerosol pollution were then compared to a run having anthropogenic sources of aerosol and both GEOS-Chem and RAMS dust sources.

2.3.4 The adsorption theory

Kumar et al. (2009) found that FHH (Frenkel, Halsey and Hill) adsorption activation theory is a far more suitable framework for describing fresh dust CCN activity than Kohler theory, based on the observed dependence of critical supersaturation, s_c , with particle dry diameter, D_{dry} . “For insoluble CCN activating according to FHH-AT, the equilibrium supersaturation of the droplet, equation is given by:

$$s_{eq} = \exp \left[\frac{4\sigma M_w}{RT\rho_w D_p} - A_{FHH} \left(\frac{D_p - D_{dry}}{2D_{H_2O}} \right)^{-B_{FHH}} \right] - 1$$

(Equation 2.1)

where σ is the CCN surface tension at the point of activation (Pruppacher and Klett, 1997), D_{dry} is the dry CCN diameter, D_{H_2O} is the diameter of water molecule equal to 2.75 Å (Kumar et al., 2009a), and A_{FHH} and B_{FHH} are adsorption parameters constrained from the activation experiments.” The CCN activation curves for dry generated dust are shown in Fig. 2.3 (Kumar et al., 2011). A simple weighting function was implemented wherein for kappa less than say 0.05 the full weight is given to the adsorption parameterization, and for kappa greater than, 0.1, zero weight is given to the adsorption parameterization and full weight given to kappa. Thus, there is a smooth transition between those regimes. Owing to their low hygroscopicity and large size, dust particles exhibit a long adsorption time scale to reach their critical supersaturation (S_c). Therefore in Setup 2, we adopt the parameterization of Kumar et al. (2009; 2011) to

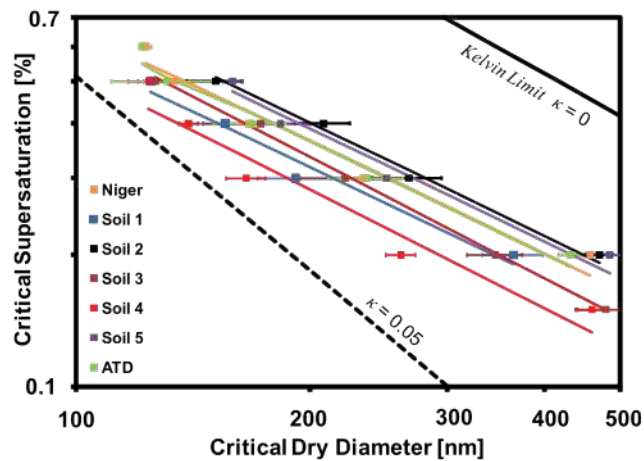


Figure 2.3: CCN activation curves of different types. Symbols show experimentally determined CCN activity and lines show FHH adsorption activation fits. Error bars represent measurement uncertainty in D_{dry} . Also shown in black thick line is the $\kappa = 0$, Kelvin curve. Black dashed line corresponds to $\kappa = 0.05$. (Figure taken from Kumar et al., 2009 with permissions)

represent adsorption effects for dust. This can result in up to 40% lower droplet concentrations than predicted by standard Kohler theory (Kumar et al., 2009). In Setup 2 we consider an external mixture of pollution aerosols, dust, and sea-spray generated sea salt, although variable sea-spray aerosols is not a focus of this study.

2.3.5 New look-up table

The original parcel model of Heymsfield and Sabin (1989) and Feingold and Heymsfield (1992) was streamlined and optimized by R. Walko. A new look-up table was constructed by Gustavo Carrio, Colorado State University from an ensemble of simulations covering a range of vertical velocity, temperature, pressure, air density, liquid water content, aerosol chemistry, aerosol size, and number concentration. In the 1st generation of this approach, aerosol chemistry was hard-wired to ammonium sulfate (Saleeby and Cotton, 2004). Subsequently the look-up tables were expanded to include aerosol chemistry represented by the hygroscopicity parameter, kappa, k ; (Ward et al., 2010). Only a single aerosol species was represented in that version.

Kinetic effects were not considered in the Ward et al scheme. The droplet activation look-up table was refined to represent an external mixture of dust, anthropogenic and natural hygroscopic aerosol, and even sea spray salt particles.

Below we list the tasks performed in relation to the adaptation and generation of a code capable of generating look-up tables (LUT's), its testing, and its implementation with RAMS:

Generalized bins describing not only particle sizes but also different hygroscopicity parameters (κ), or adsorption theory to represent dust particles were implemented. Adsorption theory (Kumar et al., 2011) was implemented for dust particles of different size; it must be noted that this expression presents singular points (for equal wet and dry particle diameters) and therefore required adaptation of an iterative scheme to find critical diameters and saturations. A control file was implemented to allow the user the selection of several characteristics defining an arbitrary number of aerosol types to be considered as well as the size partitions to represent each distribution (e.g., their hygroscopicity parameter, or dust identity, number of size bins, distribution boundaries, etc). User control files were constructed to automatically control the aforementioned code for sampling the ample parameter space required to take into account the competition of aerosols (differing in abundance and nature). The multidimensional LUT's are used to represent cloud droplet activation as well as the corresponding nucleation scavenging rates for all competing aerosol types. The newly constructed LUT consists of varying aerosol concentrations, their size distribution parameters (i.e., median diameter and width parameters), chemistry and environmental conditions (i.e., temperature, pressure, and vertical velocity).

2.3.6 Ice activation

Homogeneous ice nucleation of cloud and haze droplets is parameterized using the DeMott et al. (1994) scheme. Heterogeneous ice nucleation is parameterized using the IN-based scheme of DeMott et al. (2010) (Setup 1) or DeMott et al. (2014) for the more recent runs (Setup 2). The scheme activates IN independent of aerosol composition and instead simply relies on the total number concentration of aerosol particles greater than 0.5 μm in diameter. The sizes of the background CCN populations were too small to serve as IN, in this study. However, the fine mode dust distributions were prescribed a median radius of 0.2 μm . Assuming a lognormal size distribution, roughly 38% of these particles have diameters large enough to potentially serve as IN in the new scheme. All of the background GCCN and coarse mode dust populations were large enough to potentially serve as IN as well.

Existing parameterizations for aerosol nucleation sinks and droplet evaporation sources were adjusted to include nucleation scavenging as a sink for both dust modes, with the assumption that the largest particles are the first to nucleate. Upon droplet evaporation, the numbers of cloud1 and cloud2 droplets evaporated are added directly to the background CCN, and GCCN populations, respectively.

2.3.7 The new ice nucleation scheme

In Setup 2, the formula for ice nuclei (IN) activation was upgraded from the DeMott et al (2010) formula to the recent results reported in DeMott et al. (2014). This is because the results of the preliminary simulations suggested that dust almost completely neutralizes the effects of anthropogenic pollution aerosols on precipitation. Thus, it was decided that more confidence was needed in the representation of dust activation to form cloud droplets and ice crystals. In addition to the refinements of the approach to activation of cloud droplets by dust and hygroscopic

aerosol as discussed above, the activation of IN was refined as follows: In the DeMott et al. (2010) parameterization, the IN number concentration is a function of temperature and number concentration of dust particles greater than 0.5 microns in diameter.

$$n_{\text{INP}}(T_k) = a (273.16 - T_k)^b (n_{a>0.5\mu\text{m}})^{(c(273.16-T_k)+d)}$$

(Equation 2.2)

where $a= 0.0000594$, $b=3.33$, $c=0.0264$, $d=0.0033$, T_k is cloud temperature in degree Kelvin, $n_{a>0.5}$ is the number concentration (std cm^{-3}) of aerosol particles with diameters larger than 0.5 microns, and $n_{\text{INP}}(T_k)$ is ice nucleating particle number concentration (std L^{-1}) at T_k .

Tobo et al. (2013) observed systematic errors of predicted IN using the DeMott et al. (2010) scheme vs. measured ice particle (INP) number concentrations at a forest site dominated by biological INPs. Using the DeMott et al., (2010) in RAMS precipitation was over-predicted due to the large concentrations of ice nuclei activated. Hence, a correction factor cf was introduced in the equation based on different locations.

$$n_{\text{INP}}(T_k) = (cf) (n_{a>0.5\mu\text{m}})^{(\alpha(273.16-T_k)+\beta)} \exp(\gamma(273.16 - T_k) + \delta) \quad (\text{Equation 2.3})$$

where $\alpha=0$, $\beta= 1.25$, $\gamma= 0.46$, $\delta=-11.6$

$cf=3$ is used to estimate mineral dust IN concentration (Figure 2.4) and yields good agreement between the simplified parameterizations and the surface area based parameterization of Niemand et al. (2012). The Niemand et al. (2012) scheme was developed solely from laboratory data, supporting the atmospheric applicability of laboratory ice nucleation results to the atmosphere. Consequently, the results additionally support the premise of Niemand et al. (2012) that, to a first order, mineral dust particles from locations as separate as the Saharan or

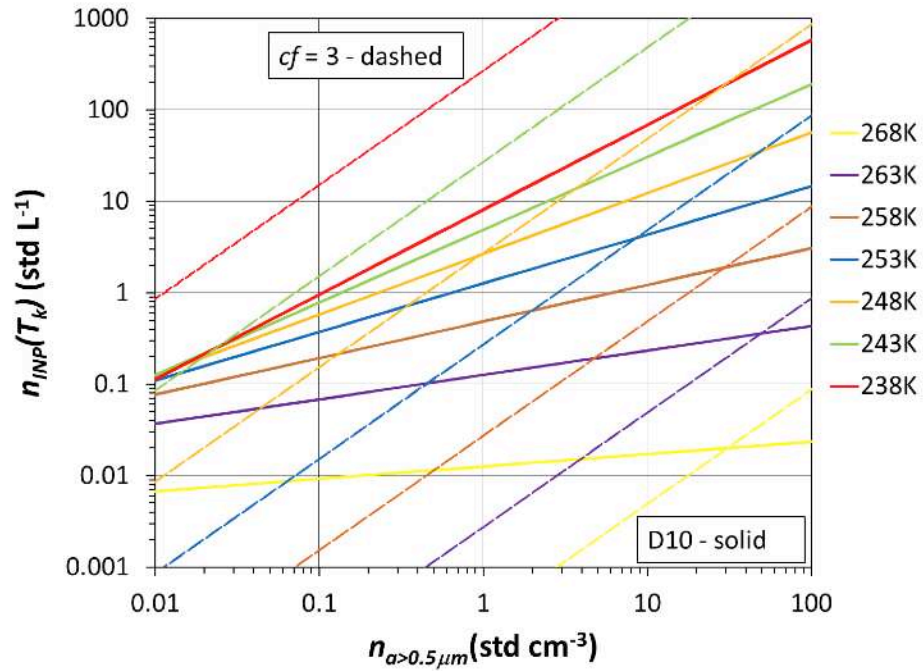


Figure 2.4: Courtesy DeMott et al., 2014; Comparison of ice nucleation parameterization with $cf=3$ with the D10 parameterization for calculations in the mixed-phase cloud regime

Asian regions may be parameterized as a common particle type for numerical modeling purposes (DeMott et al., 2014). The new scheme for ice nucleation using the DeMott 2014 ice nucleation produces fewer ice crystals in higher temperatures. DeMott 2014 is less active except for the cases when the temperatures are very cold.

2.3.8 Dust activation as GCCN

RAMS is set up to predict droplet number on only a single aerosol distribution for every grid cell and time step. This is done using the lookup table-based droplet activation scheme. The accumulation mode aerosol distributions are used in the CCN activation scheme as Aitken mode aerosols are less likely to be important in CCN prediction. The coarse mode distributions can activate at a 100% rate in a supersaturated environment (Saleeby and Cotton, 2004), as they have traditionally been assumed to have the chemical properties of sea salt. The droplet

spectrum in RAMS is composed of two cloud droplet modes and rain. The second cloud mode can be thought of as small drizzle droplets that form either from self-collection among droplets in the first cloud mode or nucleation of giant GCCN. GCCN are considered aerosol particles greater than 1 μm (or coarse mode aerosol particles) that are wettable. In earlier versions of RAMS it was assumed that all wettable particles (like mineral dust) greater than 1 μm would form droplets in the second cloud mode whenever the relative humidity exceeded 100% (Saleeby and Cotton, 2004; Ward and Cotton, 2010). Lerach (2012) examined this hypothesis with a range of updraft speeds, by performing parcel model simulations for dust in moist rising air with an assumed κ value of 0.03. For a given chemical composition, Köhler theory predicts that the dry particle size increases with the decrease in critical supersaturation, making it easier to activate larger particles. This is a result of the fact that the Kelvin curvature effect is very small for such large particles. Lerach (2012) found that the activation fraction for dust particles greater than 1 μm reaches 100% for updraft speeds greater than 2.87 m/s and reduces appreciably for speeds less than 0.01 m/s.

2.3.9 Precipitation scavenging

Precipitation scavenging of aerosols and sea-salt particles in RAMS is dependent on the moments of each size spectra of precipitating liquid species (i.e., drizzle and rain). Scavenging coefficients are computed separately for CCN, GCCN as well as the film, jet, and spume sea-salt modes. The scheme is based on empirical data (Chate et al., 2003, 2007) linking scavenging coefficients to rainfall rates at every model grid cell (computed from the drizzle and raindrop spectra). This helps in the reduction of the uncertainty linked to drop-particle collision efficiencies.

2.4.0 RAMS dynamic model setup

In this study we set up the Colorado State University (CSU) Regional Atmospheric Modeling System (RAMS) version 6.0. Table 2.1 summarizes the features of the RAMS setup for this study. Figure 2.5 shows the grid configuration used. The outermost grid, Grid 1 has 36 km grid spacing and consists of almost all of North America. Grid 2 is displayed in the blue color and has a grid spacing of 12 km. The innermost grid is Grid 3, displayed in red with a grid spacing of 3 km. The topography of the domain is displayed in Figure 2.6. The 32km North American Regional Reanalysis (NARR) (Mesinger et al., 2006), was used for model initialization and boundary nudging of the geopotential height, temperature, relative humidity, and winds on grid-1 and the radiative boundary condition of Klemp and Wilhelmson (1978) was applied to the lateral boundaries. RAMS has an upper boundary condition that acts as a rigid lid, with a wave absorbing high-viscosity layer aloft used in the top most model levels to absorb gravity waves, by nudging to large-scale analysis or initial conditions (Cotton et al., 2003).

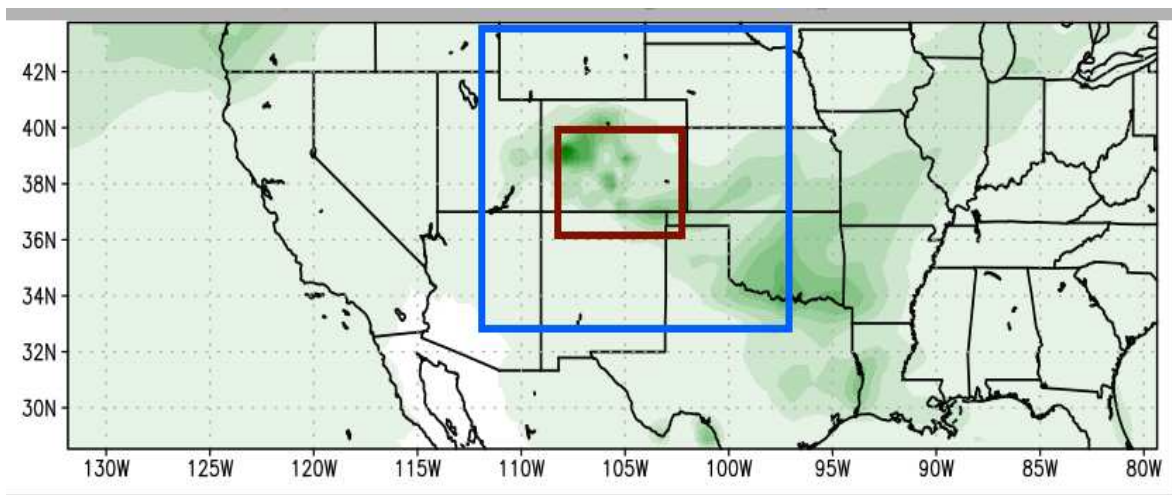


Figure 2.5: The 3 grid configuration is shown here. Grid 1 has the 36 km grid spacing and comprises of the entire outer boundary in the map. Grid 2 is 12 km and is shown in blue rectangle. Grid 3 is of 3 km spacing and is displayed in red rectangle.

We examine the cumulative effect of dust and pollution aerosol acting as cloud nucleating aerosol (CCN, GCCN, IN) over the entire Colorado Rocky Mountains for the months of October 2004 to mid- April 2005 (Water Year 2005). We differ from Saleeby et al. (2011), by choosing months covering the entire snow year. The entire winter season analysis provides a range of seasonal conditions, snowfall totals and variability in dust production and anthropogenic aerosol. Two setups of snow season long simulations are performed. The first set up (Setup 1), is composed of the original Lerach (2012) look-up table for cloud droplet activation and the DeMott et al. (2010) IN activation scheme. After completion of the Setup 1 simulations, it was found that dust enhanced precipitation almost exactly in opposition to reduction in precipitation by pollution aerosol. Because of the small combined effect of dust and pollution aerosol, it was decided to re-run the season-long simulations using DeMott et al. (2014) IN activation scheme and the most recent version of the CCN activation look-up table. This will tell us how sensitive the results are to modest variations in cloud microphysics and also tell us how robust the results are. Both these schemes were tested for two different kinds of dust and aerosol environments which are as follows; a) ‘clean’ runs, where the regional dust sources were turned off and only non-anthropogenic dust and aerosol sources from the GEOS-Chem were considered. b) ‘dirty’ in which the dust sources from RAMS were turned ON to represent the regional dust sources and anthropogenic dust and aerosol were nudged from GEOS-Chem into the RAMS to represent the long range transport of dust into the model as well as the effects of anthropogenic aerosol.

Time step	30 s
Simulation duration	6.5 months
Microphysics scheme	Setup1 :Two-moment bin-emulating microphysics (Saleeby and Cotton 2004, 2008, 2009) DeMott et al., 2010 heterogeneous ice nucleation Water species: vapor, cloud1 and cloud2 drops, rain, pristine ice, snow, aggregates, graupel, and hail Setup2: As in Setup 1 but DeMott et al., 2014 heterogeneous ice nucleation, and new lookup table including adsorption theory for dust (Kumar et al., 2011) Setup 3: same as Setup 2 with dust sources also present in the non-anthropogenic control run
Aerosol & Dust Sources	GEOS-CHEM and RAMS regional dust sources
Boundary conditions	Radiative lateral boundary (Klemp and Wilhelmson, 1978a) Top: Rigid lid with a high-viscosity layer aloft to damp gravity waves, by nudging to large-scale analysis or initial conditions (Cotton et al., 2003)
Turbulence scheme	Mellor and Yamada, 1974; level 2.5 scheme on grids 1-3; Smagorinsky, 1963; The Kain and Fritsch, 1993 cumulus parameterization applied to grids 1 and 2, convection was resolved explicitly on grid 3.
Radiation scheme	Harrington, 1997; with additions from Stokowski, 2005
Surface scheme	LEAF-3 (Walko et al., 2000)

(GEOS), including wind, convective mass fluxes, mixed layer depths, temperature, clouds, precipitation and surface properties. The aerosol simulation in the GEOS-Chem includes the sulfate-nitrate-ammonium system (Park et al., 2004; 2006), carbonaceous aerosol (Park et al., 2003; Liao et al., 2007). Sea-spray emissions are estimated using the Clarke et al. (2006) scheme, and dust emissions are estimated using the Ginoux et al. (2001) scheme. Both wet and dry depositions are included (Liu et al., 2001) through washout and rainout. GEOS-Chem is configured with 47 vertical levels and run with a horizontal resolution of $0.5^\circ \times 0.667^\circ$. GEOS-Chem was run with a spin-up of about 1 month.

The smallest size bin of dust, DST1 (0.1-1 microns) is introduced into the RAMS code. The appropriate modifications have been done in the microphysics subroutine and new subroutines have been added to read dust into RAMS. Dr. Jeffery Pierce of Colorado State University ran GEOS-Chem and provided the output data. The data obtained is post processed by using the panoply software, obtained from NASA (<http://www.giss.nasa.gov/tools/panoply/>). Standard GEOS-Chem simulations include ~60 gas and aerosol-phase species. The aerosol species simulated are sulfate, nitrate, ammonium, hydrophobic organics, hydrophilic organics and dust. Emissions of gases and aerosols are discussed in Wainwright et al. (2012). Aerosols introduced into RAMS are 3 lumped species: inorganic species, hydrophilic organics and hydrophobic organics. The concentrations of these species in RAMS are nudged from aerosol concentrations in GEOS-CHEM. The pollution aerosol data that has been taken from the GEOS-Chem model consists of 13 different species. The aerosol data consist of a sum of hydrophobic and hydrophilic black carbon and organic aerosol, hydrophilic organics which consists of SOAs (lump of aerosol products of first 3 (ALPH + LIMO + TERP) hydrocarbon oxidation, aerosol production of ALCO oxidation, aerosol production of SESQ oxidation, aerosol production of ISOP oxidation, aerosol production of aromatics oxidation). The inorganic aerosol consists of the sum of nitrate, sulfate and ammonium and has a characteristic kappa-value of 0.6. The hygroscopic organic aerosols contain (hydrophilic black carbon, hydrophilic organic carbon and the five SOA species) and have a kappa-value of 0.12. The hydrophobic aerosols (hydrophobic black carbon and hydrophobic organic carbon) have a kappa-value of 0.0. The seasonal average variation of dust and pollution aerosol concentration has been plotted in Figure 2.7 and 2.8.

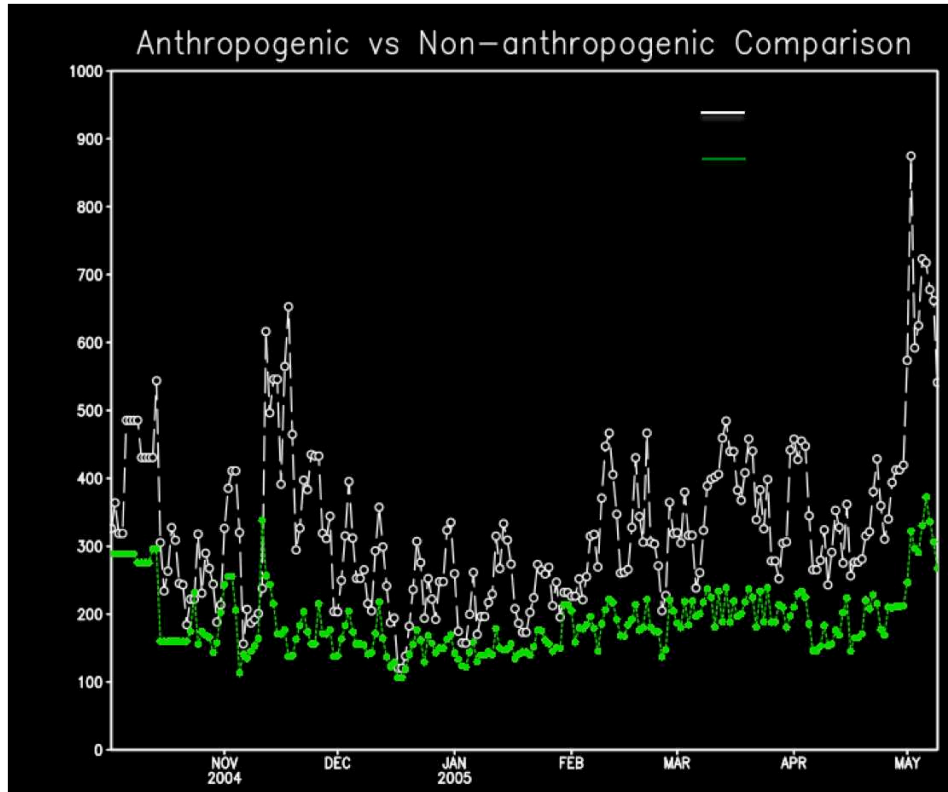


Figure 2.7: Concentration of aerosol for the entire season

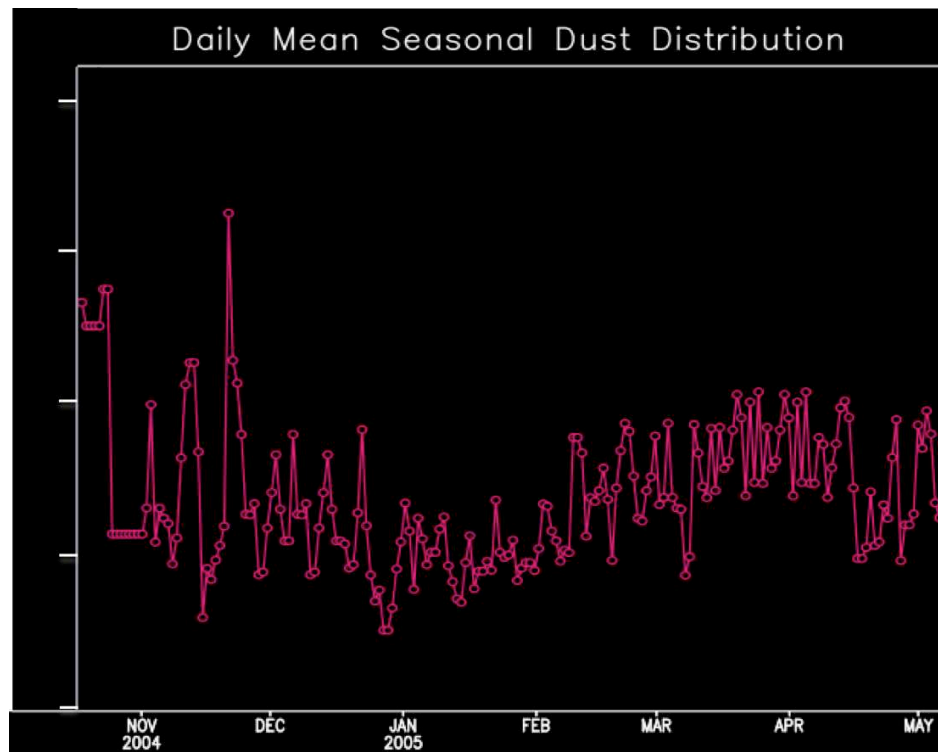


Figure 2.8: Concentration of dust for the entire season

2.6.0 Model Results

The simulations were run with both the old (Setup 1) and new code (Setup 2) for the ‘clean; and ‘dirty’ runs. Setup1 had Lerach’s scheme for droplet activation and the DeMott et al., (2010) for IN activation. Setup 2 has the more recent runs with the newer lookup table including adsorption effects, and competition among externally mixed aerosol species, and the DeMott et al., 2014 scheme for heterogeneous nucleation of ice. Since the results with the old scheme showed very small effects, it was decided to rerun with “improved” estimates. Simulations for a period of 6 months were run for the entire region and the runs were re-initialized for each 10-day period. Each of the individual ten-day periods was analyzed separately. It was observed that for each period a non-monotonic response was represented. An increase or decrease of precipitation depended on the concentration of dust and CCN pollution, which governed the particular phase (Table 2.1). The periods that experienced an increase in the precipitation were the ones, which were dominated by high dust concentrations ($\sim 100/\text{cm}^3$) and low CCN concentrations ($\sim 200/\text{cm}^3$) (Figure 2.9, 2.10). The periods that exhibited a decrease in the precipitation had higher CCN concentration ($\sim 2000/\text{cm}^3$) for the ten days of run and the dust concentrations were lower for the same period ($\sim 30/\text{cm}^3$). However, this was not the sole factor and meteorological drivers like high wind speed, cloud base heights and cloud base temperatures and wet or dry system had larger influences on the precipitation change which was later found out through the sensitivity study results (Figure 2.11, 2.12). Cloud droplet diameters decreased after the period of CCN peak, which is consistent with the concept that high CCN concentration leads to more numerous droplets, which are smaller in diameter (Figure 2.13, 2.14). Similar patterns were found for the other periods which experienced an increase or decrease in precipitation (Figure

Table 2.2: Comparison of integrals precipitation per period for setup 1

Period	Clean	Dirty	Difference
1	3.66E+13	3.98E+13	8.82%
2	2.08E+13	2.07E+13	-0.51%
3	2.67E+13	2.93E+13	9.84%
4	1.30E+13	1.31E+13	0.50%
5	3.35E+13	3.39E+13	1.38%
6	2.36E+13	2.35E+13	-0.47%
7	1.22E+13	1.22E+13	-0.47%
8	7.32E+12	7.22E+12	-1.39%
9	1.55E+13	1.55E+13	0.18%
10	3.14E+13	3.14E+13	7.07E-04
11	1.71E+13	1.69E+13	-0.95%
12	2.24E+13	2.28E+13	1.91%
13	2.41E+13	2.40E+13	-0.37%
14	2.10E+13	2.11E+13	0.52%
15	3.84E+13	3.63E+13	-5.47%
16	2.47E+13	2.48E+13	0.49%
17	2.33E+13	2.34E+13	0.19%
18	3.83E+13	3.85E+13	0.41%
19	1.77E+13	1.74E+13	-1.81%
20	1.99E+13	1.99E+13	-8.67E-04

2.15-2.18). The interplay between high concentrations of hygroscopic aerosol and high concentrations of dust is interesting. High concentrations of hygroscopic aerosol results in higher concentrations of droplets, and for a given amount of liquid water, the droplets are smaller, and riming efficiencies are less, and they expose greater surface area than fewer bigger droplets. In the presence of high concentrations of dust, which serve as IN, greater concentrations of ice crystals occur. These more numerous ice crystals grow by the Wegener Bergeron Findeisen (WBF) process, which proceeds more efficiently in the presence of the smaller cloud droplets, which exhibit enhanced surface area (other things being the same). Thus precipitation is enhanced during the dusty periods, unless dust concentrations are too high (See Part II).

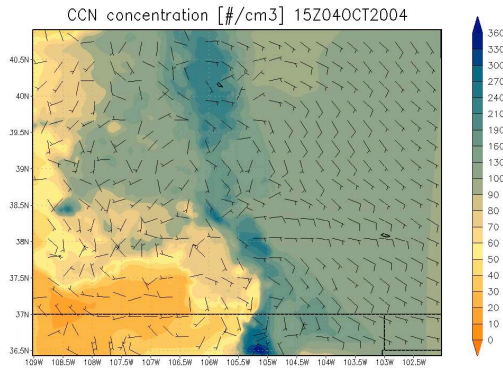


Figure 2.9: CCN concentration for period 1

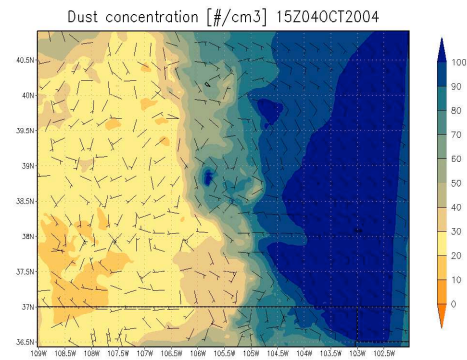


Figure 2.10: Dust concentration for period 1

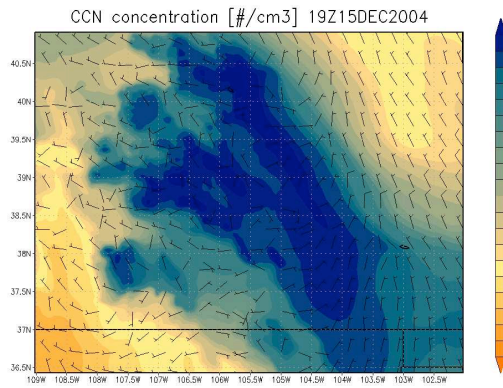


Figure 2.11: CCN concentration for period 8

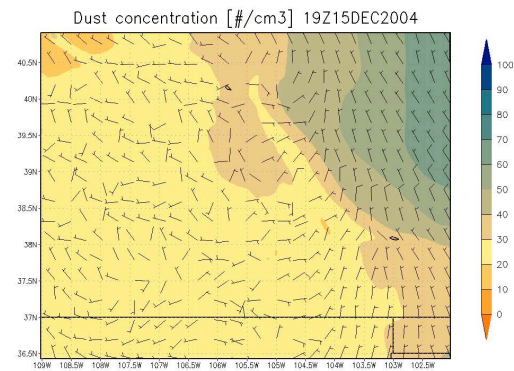


Figure 2.12: Dust concentration for period 8

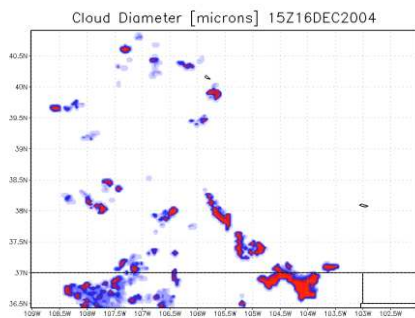


Figure 2.13: Cloud diameter before the CCN peak for period 8

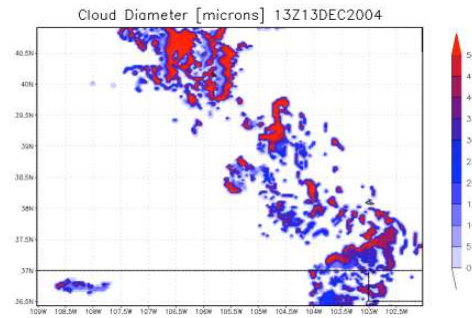


Figure 2.14: Cloud diameter after the peak for CCN peak for period 8

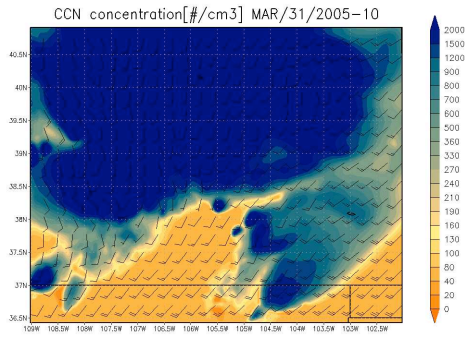


Figure 2.15: CCN concentration for period 19

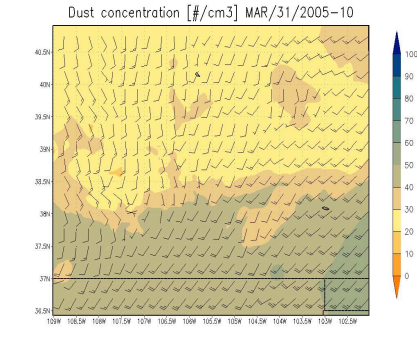


Figure 2.16: Dust concentration for period 19

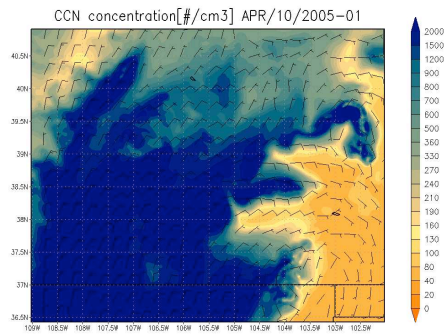


Figure 2.17: CCN concentration for period 20

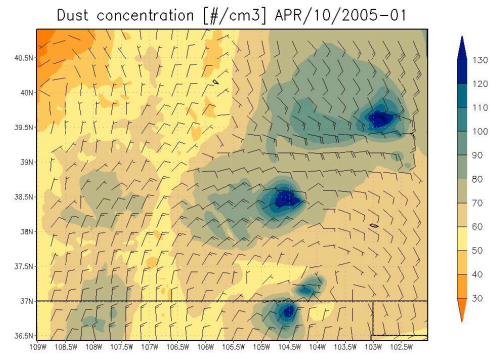


Figure 2.18: Dust concentration for period 20

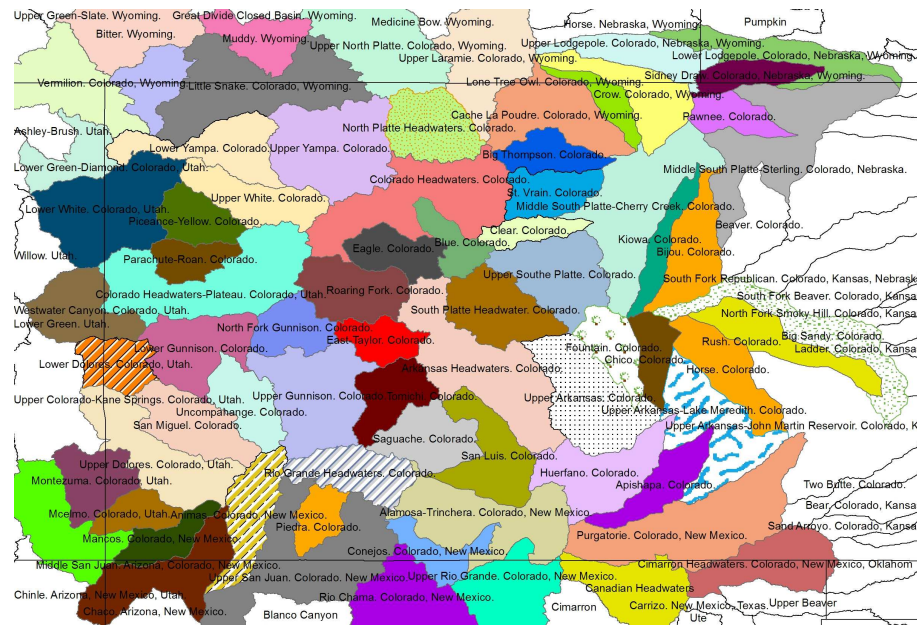


Figure 2.19: Map for the regions for different river basin

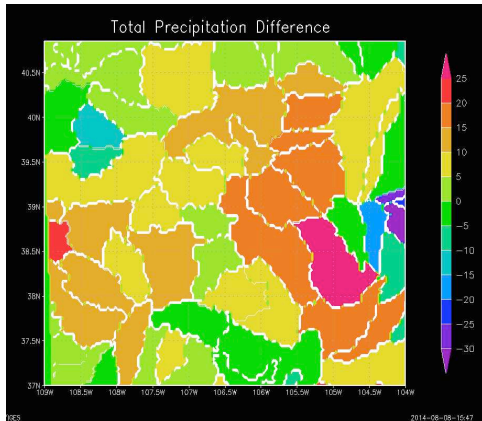


Figure 2.20: Map for precipitation difference in both regions for different river basins in % for Period 1

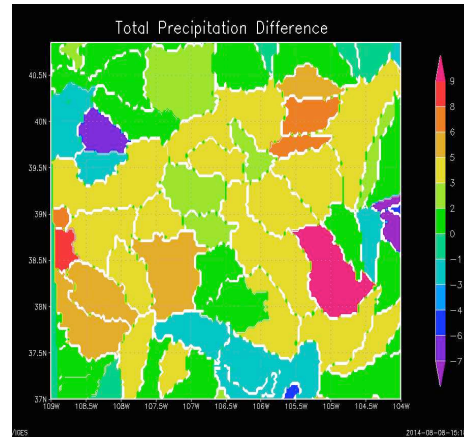


Figure 2.21: Map for Precipitation difference in both regions for different river basin in % for the entire season

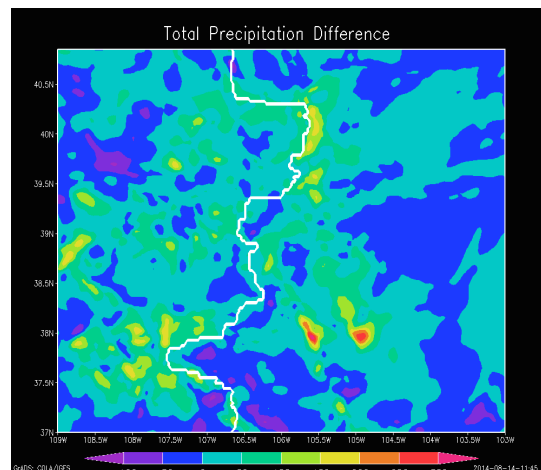


Figure 2.22: Integral mass of precipitation difference in both regions setup 1

The Colorado River basin comprises 71 different basins (Figure 2.19). Figure 2.20 shows the map for precipitation difference in both regions for the different river basins in % for the period 1 in the Table 2.2, which experiences an increase in precipitation because of the high dust

concentration. However, for Setup 1, the map for precipitation difference in both regions for different river basin shows a less significant increase for all the periods because it is averaged over periods of high CCN concentration, which lowers the precipitation (Figure 2.21). Figure 2.22 shows the difference in the integral mass of precipitation for both regions, with the white line signifying the Atlantic divide in the map. For the setup 1, a small decrease of $\sim 0.1\%$ for the CRB is predicted. An increase of $\sim 0.28\%$ in the leeward side is seen which suggests a slight precipitation spill-over effect. The difference in precipitation for the basins has been shown in the table A.1 in the appendix. These were the results obtained from the Setup 1 code. Since the results with Setup 1 showed very small effects, it was decided to rerun with “improved” estimates.

2.7.0 Conclusions

The Setup 1 simulation results show a small decrease of $\sim 0.1\%$ for the CRB. Precipitation increases by $\sim 0.28\%$ in the leeward side of the mountains by the ‘spillover effect’. The combined effect of dust and pollution aerosol is a slight decrease in the precipitation in the CRB, with dust largely offsetting the spillover effects of aerosol pollution. Dust mainly effects wintertime orographic precipitation in these low supersaturation clouds by serving as IN. Because the results of the seasonal simulations from Setup 1 suggest that seasonal precipitation amounts are a very small difference between two relatively large competing effects it was decided to refine the droplet and ice activation codes, as discussed in Section 2.3.6 above.

The RAMS simulation for the same period (October 2nd-April 20th) was run using Setup 2, which has the DeMott et al. (2014) droplet nucleation scheme for heterogeneous nucleation of ice, adsorption theory for the representation of dust nucleation (Kumar et al., 2010) and the updated look up table discussed above. It was found that total integral precipitation decreases by

2.32 % for the Grid 3 and it decreases 1.9 % for the CRB. The difference in precipitation for both regions has been shown in Figure 2.23. Figure 2.24 shows the shift in precipitation with respect to each river basin. The total precipitation loss occurred in the Grid 3 area (Figure 2.25) using the Setup 2 code is 6,070,000 acre feet of water for the 6.5 months of simulation, and is 4,020,000 acre feet for the CRB.

2.8.0 Discussion

The 500-hPa geopotential height fields display zonal flow over Colorado and southwesterly flow over the Southwest part of the state and an averaged trough condition is seen

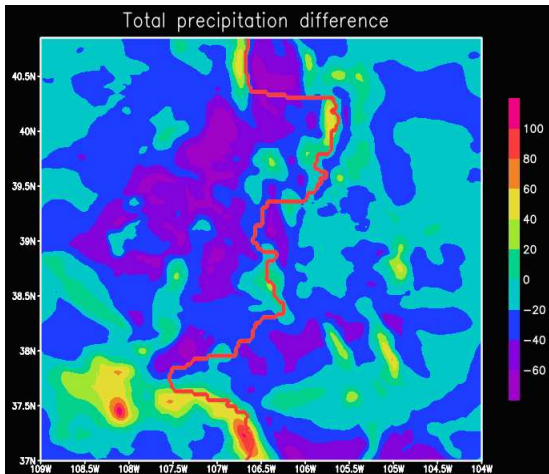


Figure 2.23: Map for precipitation difference in both regions using setup 2

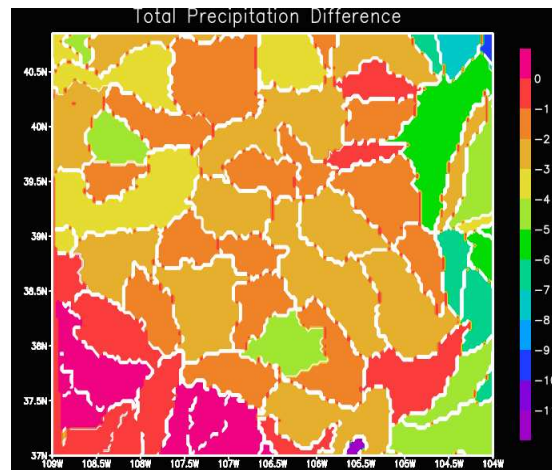


Figure 2.24: Map for precipitation difference in both regions for different river basins using the setup 2

offshore southern California (Figure 2.26). From the geopotential height anomaly field there is a greater persistence in 2005 for low pressure systems over the Southwest (Figure 2.27). It is evident from the relative humidity fields that 2005 water year (WY) was a moist year (Figure 2.28). The mean height field and moisture patterns support the tendency for heavy snowfall in 2005 with higher precipitation in southwest Colorado region. These synoptic conditions have an important impact on the snowfall variation and can affect the response of these cloud systems in

terms of precipitation changes due to dust and aerosol pollution.

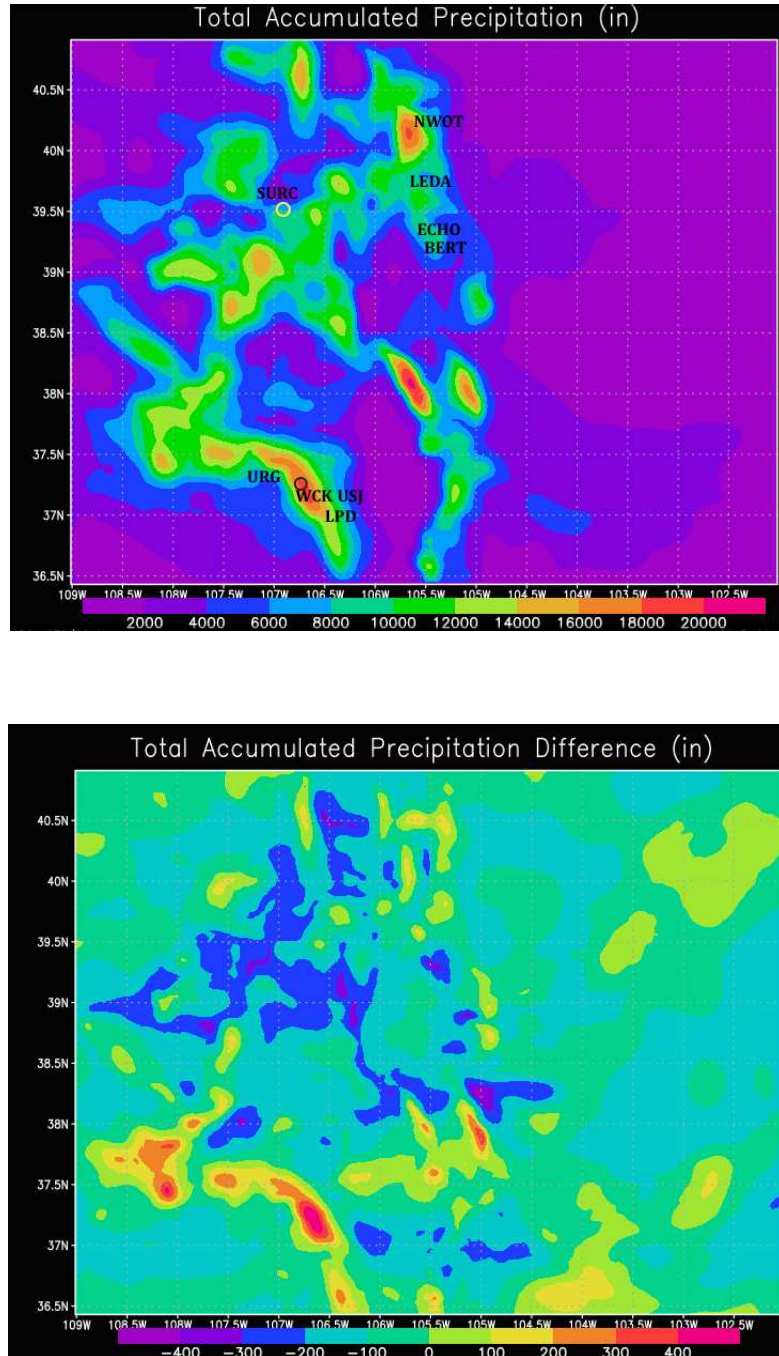


Figure 2.25: Top: Total accumulated precipitation for the grid 3. Bottom: total accumulated precipitation difference in inches for Setup 2

2.8.1 Snotel observation and comparisons

All numerical models are subject to different degrees of variability and their predictions are limited by this factor (Wetzel et al., 2004). The time series of the Snow Water Equivalent (SWE) for the seasonal trend of precipitation was compared with Snotel site observational measurements. We selected Snotel sites closest to RAMS grid points and made comparisons with a group of Snotel sites around a selected point. RAMS tends to over-predict precipitation in most of the cases. However, in some cases there were instances of under-prediction by RAMS as well (Figure 2.29, 2.30). The Wolf Creek Snotel site (lat: 37.29, lon: -106.48) measured the highest precipitation and Upper Rio Grande (URG) (lat: 37.43; lon: -107.46) measured the lowest precipitation. Saleeby and Cotton (2005, 2008) demonstrated that the CSU RAMS performs rather well in winter snowfall prediction for individual cases over the Park Range with a tendency for over-prediction in some individual events (Saleeby et al., 2010). The variability might be attributed to location of the grid cells and the abrupt terrain change between grid cells. Hence, it is important to well represent the terrain in the sigma Z terrain following system (Saleeby et al., 2010). RAMS in general, does a fair job of predicting the precipitation. The differences in plots are because of the differences in location of Snotel sites. Some of the Snotel sites have a lapse in observation on days when the instruments get covered by snow and sometimes there is blowing over of snow by high wind events which might result in RAMS appearing to over –predict.

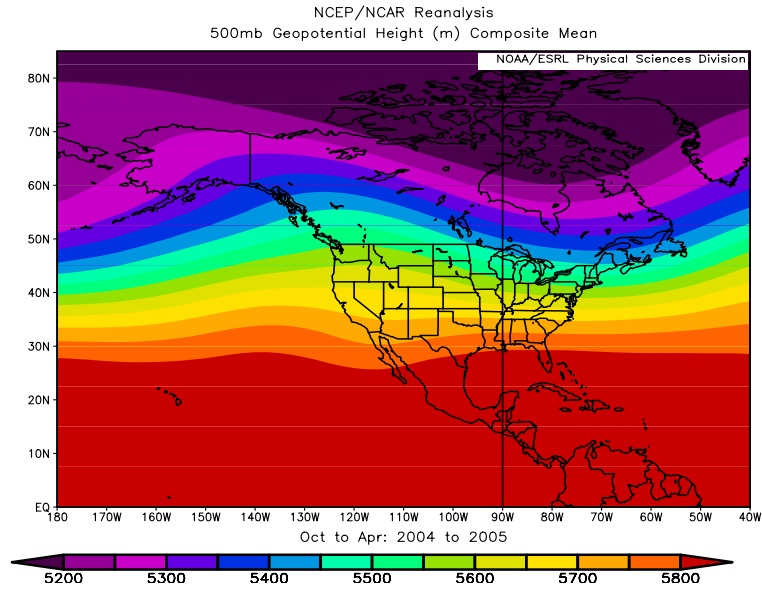


Figure 2.26: Composite 500-hPa geopotential height (m) from the NARR dataset for 1 Oct-Apr 2005

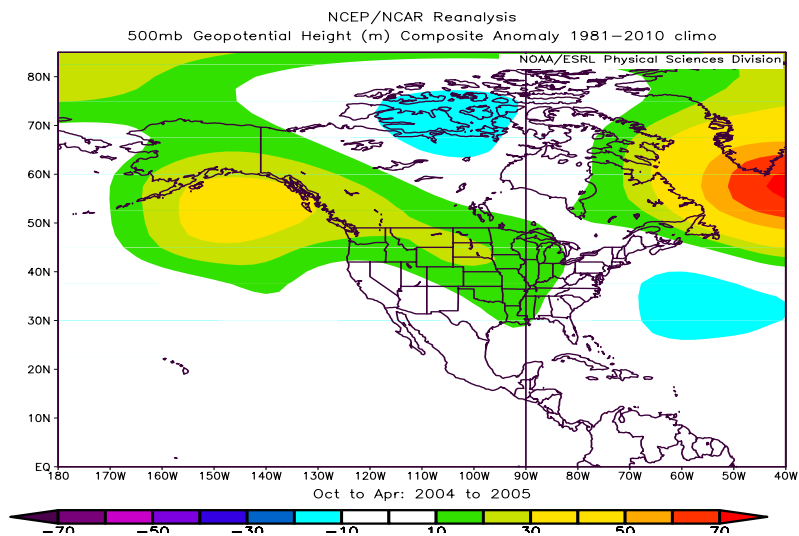


Figure 2.27: Composite 500-hPa geopotential height anomaly from the NARR dataset for 1 Oct-Apr 2005

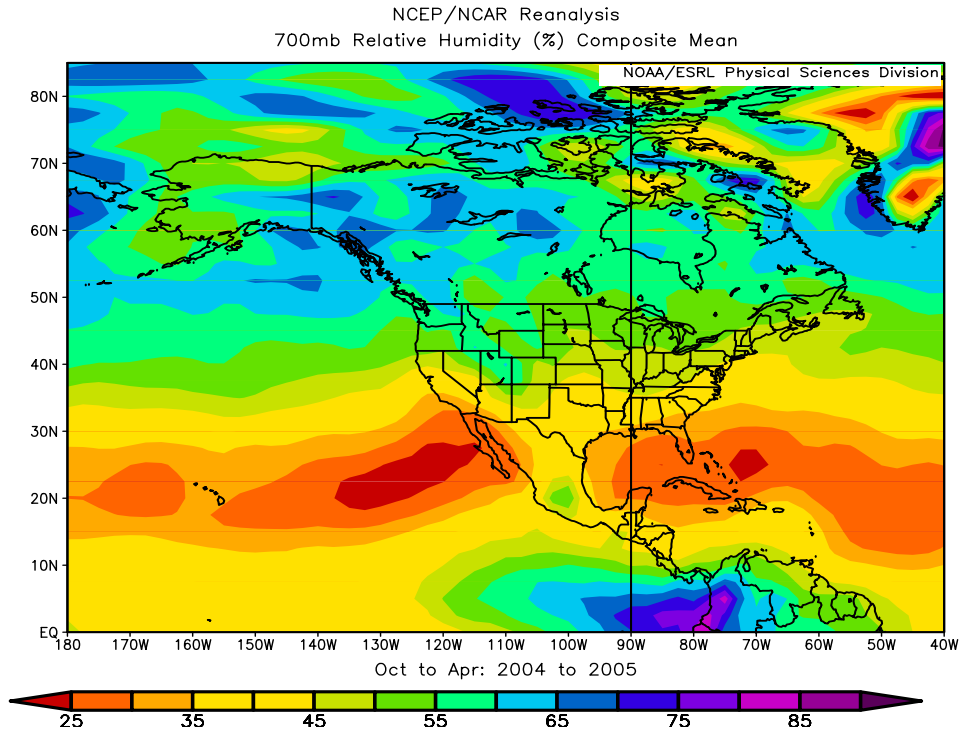


Figure 2.28: 700-hPa RH anomaly (%) from the NARR dataset for 1 Oct- Apr 2005

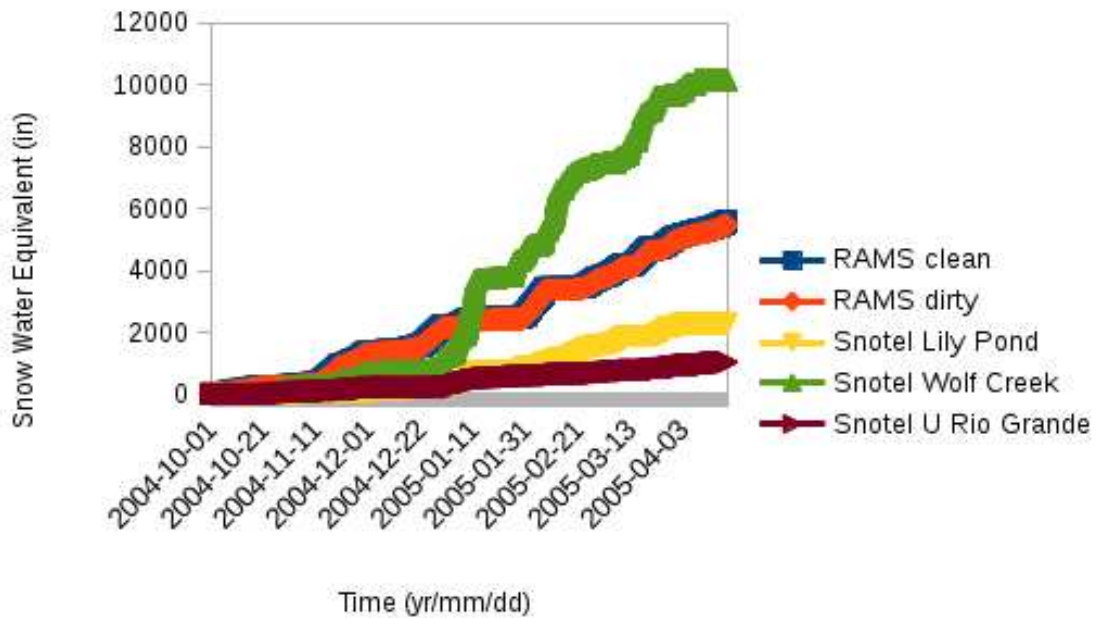


Figure 2.29: Total accumulated Comparison of RAMS precipitation with Snotel sites

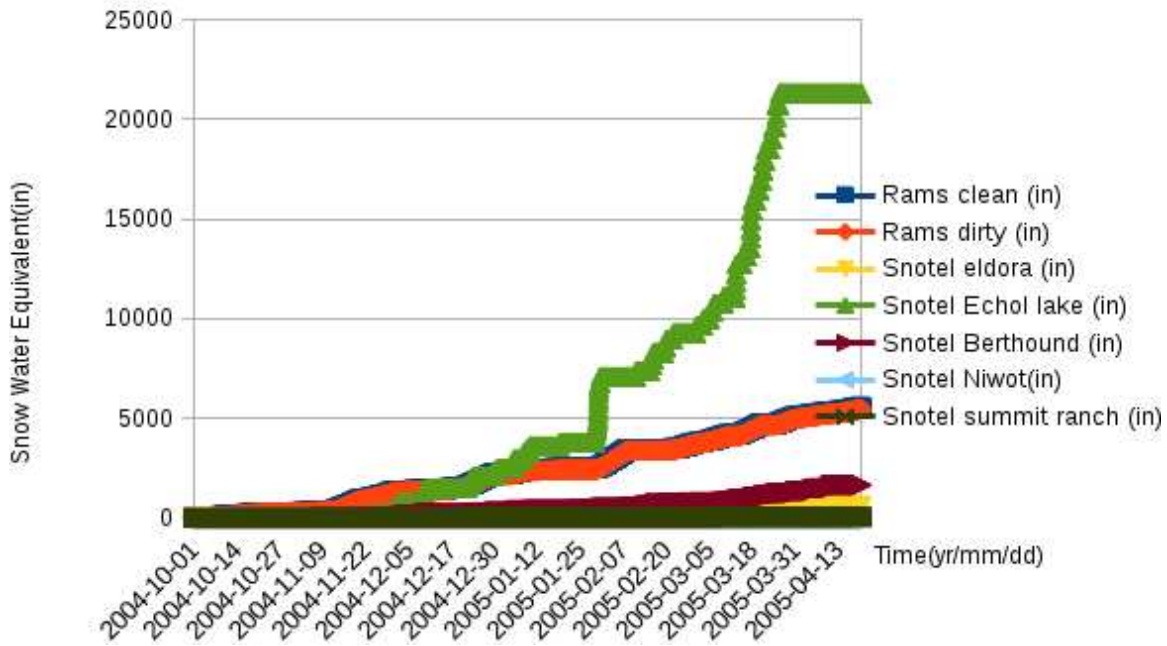


Figure 2.30: Total accumulated Comparison of RAMS precipitation with Snotel sites

2.8.2 Summary

Several modeling studies, Saleeby and Cotton (2005) and Saleeby et al. (2006, 007, 2009, 2010) examined the impact of increasing hygroscopic aerosol concentration on the resulting snowfall during winter weather events in 2004-2007. They concluded that the high aerosol concentrations impede the process of riming and therefore results in unrimed or lightly rimed ice hydrometeors (Saleeby et al., 2010). This work is a follow-up modeling study where the combined impact of dust and aerosol pollution has been examined for the water year 2005. The Colorado State University Regional Atmospheric Modeling System (Cotton et al., 2003; Saleeby and Cotton, 2004; 2008; 2010) was used to simulate winter snowfall events from 1 October 2004 to 20 April 2005 within a nested grid framework at a grid spacing of 3 km. For the WY 2005, two sets of simulations were run, clean and dirty. This was performed using two different sets of codes (Setup 1 and Setup 2). The clean simulations had only non-anthropogenic

pollution aerosols and no long range transported dust sources, or RAMS regional dust sources. The dirty simulations had anthropogenic sources of aerosol pollution and long range transported dust represented by nudging the GEOS-Chem data and regional RAMS-predicted dust sources. It was concluded that the seasonal precipitation variations consist of multiple episodes, which, in turn, impact the long term average.

Although dust acting as IN tends to increase precipitation for individual events; the total precipitation change over the season is largely ruled by aerosol pollution, which has opposing impact to dust. The net change in domain total integral precipitation, using the updated code (Setup 2) on the Colorado 3-km grid spacing domain, resulting from an increase in aerosols and dust pollution was a reduction of 2.32 % for the Grid 3 and a decrease in 1.9 % for the CRB. This corresponds to total winter-season precipitation loss of 4,020,000 acre-feet of water for the 6.5 months of simulation for the CRB. Owing to the use of adsorption theory in Setup 2, dust impacts on CCN activation are less, yielding a slight decrease in season-long precipitation. This can be attributed to dust activation being represented by adsorption theory. This suggests that Setup1 which is solely based on Kohler theory over-predicts dust activation as CCN. Moreover, the DeMott et al. (2014) IN activation scheme produces fewer ice crystals than the DeMott et al. (2010) scheme thus Setup 2 results in lesser amounts of dust enhancement of precipitation. The adsorption effects should mean dust does not reduce precipitation as much and since the DeMott et al. (2014) formula produces fewer IN than DeMott et al. (2010) then this largely explains the difference.

Setup 3, is similar to Setup 2 with dust sources present in the non-anthropogenic control run. Since anthropogenic sources of dust occur tend to be less than non-anthropogenic sources, this was done for reevaluating the dirty runs ((Huang et al., 2015; Ginoux et al., 2001). In this set

of runs, the non-anthropogenic aerosol was turned ON. The local dust sources were turned ON from RAMS dust model as well as the dust from the GEOS-Chem was also turned ON and nudged into the RAMS. This represented both coarse (local dust sources) and the fine mode dust particles (long range transport). The clean background or non-anthropogenic sources of aerosol pollution were then compared to a run having anthropogenic sources of aerosol and both GEOS-Chem and RAMS dust sources.

It was found that the net change in domain total integral winter-season precipitation using Setup 3 was a reduction of precipitation 2.56 % for the Grid 3 and a decrease in 2.1 % for the CRB compared to the run with no anthropogenic aerosol sources. This corresponds to total winter-season precipitation loss due to anthropogenic pollution of 5,380,00 acre-feet of water for the 6.5 months of simulation for the CRB.

In addition to this, synoptic patterns and meteorological conditions outweigh the microphysical parameters. However, it is important to assess the human based changes that impact the snowfall over a mountainous region for better understanding of the microphysical feedback and the overall change.

REFERENCES

- Albrecht, B., 1989. Aerosols, cloud microphysics, and fractional cloudiness. *Science*, 245, 1227–1230.
- Benoit, L., Beatrice, M., Gilles, B., Chazette, Maig P., Schmechtig, C., 2005. Simulation of the mineral dust emission frequencies from desert areas of China and Mongolia using an aerodynamic roughness length map derived from the POLDER/ADEOS 1 surface products. *J. Geophys. Res.* 110, D18S04.
- Chate, D. M., Rao, P. S. P., Naik, M. S., Momin, G. A., Safai, P. D., Ali, K., 2003. Scavenging of aerosols and their chemical species by rain. *Atmos. Environ.* 37, 2477–2484.
- Cotton, W. R., Pielke Sr., R. A., Walko, R. L., Liston, G. E., Tremback, C. J., Jiang, H., McAnelly, R. L., Harrington, J. Y., Nicholls, M. E., Carrio, G. G., McFadden, J. P., 2003. RAMS 2001: Current status and future directions. *Meteor. Atmos. Phys.* 82, 5–29.
- Cotton, W. R., Pielke, R. A., 2007. Human impacts on weather and climate. Cambridge University Press, 330 pp.
- DeMott, P. J., Möhler, O., Stetzer, O., Vali, G., Levin, Z., Petters, M. D., Murakami, M., Leisner, T., Bundke, U., Klein, H., Kanji, Z., Cotton, W. R., Jones, H., Benz, S., Brinkmann, M., Rzesanke, D., Saatho, H., Nicolet, M., Saito, A., Nillius, B., Bingemer, H., Abbatt, J., Ardon, K., Ganor, E., Georgakopoulos, D. G., Saunders, C., 2011. Resurgence in ice nucleation research. *B. Am. Meteorol. Soc.* 92, 1623–1635.
- DeMott, P. J., Meyers, M. P., Cotton, W. R., 1994. Parameterization and impact of ice initiation processes relevant to numerical model simulations of cirrus clouds. *J. Atmos. Sci.* 41, 77-90.
- DeMott, P. J., Petters, M. D., Prenni, A. J., Carrico, C. M., Kreidenweis, S. M., Collett, J. L., Moosmuller, H., 2009. Ice nucleation behavior of biomass combustion particles at cirrus temperatures. *J. Geophys. Res.* 114, D16205, doi: 10.1029/2009jd012036.
- DeMott, P. J., Prenni, A. J., Liu, X., Petters, M. D., Twohy, C. H., Richardson, M. S., Eidhammer, T., Kreidenweis, S. M., Rogers, D. C., 2010. Predicting global atmospheric ice nuclei distributions and their impacts on climate. *P. Natl. Acad. Sci. USA*, 107, 11217–11222.
- DeMott, P. J., Sassen, K., Poellot, M. R., Baumgardner, D., Rodgers, D. C., Brooks, S. D., Prenni, A. J., Kreidenweis, S. M., 2003. African dust aerosols as atmospheric ice nuclei. *Geophys. Res. Lett.* 30, 1732, doi:10.1029/2003GL017410.
- Feingold, G., Kreidenweis, S. M., Zhang, Y., 1998. Stratocumulus processing of gases and cloud condensation nuclei: Part I: trajectory ensemble model. *J. Geophys. Res.* 103, 19527–19542.
- Gagin, A., 1965. Ice Nuclei, their physical characteristics and possible effect on precipitation initiation: Proc. Tokyo-Sapporo Int. Conf. On Cloud Physics, Sapporo, Japan, Int. Assoc. of Meteor. and Atmos. Phys. of the IUGG. 155-162.
- Ginoux, P., Chin, M., Tegen, I., Prospero, J. M., Holben, B., Dubovik, O., Lin, S. J., 2001. Sources and distributions of dust aerosols simulated with the GOCART model. *J. Geophys. Res.* 106, 20255–20274.

- Harrington, J. Y., 1997. The effects of radiative and microphysical processes on simulated warm and transition season Arctic stratus. Ph.D. dissertation, Atmospheric Science Paper 637, Dept. of Atmospheric Science, Colorado State University, 289 pp.
- Heymsfield, A. J., Sabin, R. M., 1989. Cirrus crystal nucleation by homogeneous freezing of solution droplets. *J. Atmos. Sci.* 46, 2252–2264.
- Hung, H. M., Malinowski, A., Martin, S. T., 2003. Kinetics of heterogeneous ice nucleation on the surfaces of mineral dust cores inserted into aqueous ammonium sulfate particles. *J. Phys. Chem.* 107, 1296-1306.
- Huang, J. P., Liu, J. J., Chen, B., Nasiri, S. L., 2015. Detection of anthropogenic dust using CALIPSO lidar measurements. *Atmos. Chem. Phys.* 15, 11653-11665.
- Isono, K., Komabayasi, M., Ono, A., 1959. Volcanoes as a source of atmospheric ice nuclei. *Nature.* 183, 317-318.
- Kain, J. S., Fritsch, J. M., 1993. Convective parameterization for mesoscale models: The Kain–Fritsch scheme, in: Emanuel, K. A., et al., (eds.), *The Representation of Cumulus Convection in Numerical Models*. Meteor. Monogr. 24, Amer. Meteor. Soc., 165–170.
- Klemp, J. B., Wilhelmson, R. B., 1978. Simulations of right-and left-moving storms produced through storm-splitting. *J. Atmos. Sci.* 35, 1097-1110
- Koehler, K. A., Kreidenweis, S. M., DeMott, P. J., Petters, M. D., Prenni, A. J., Carrico, C. M., 2009. Hygroscopicity and cloud droplet activation of mineral dust aerosol. *Geophys. Res. Lett.* 36, L08805, doi:10.1029/2009GL037348.
- Kumar, P., Nenes, A., Sokolik, I. N., 2009. Importance of adsorption for CCN activity and hygroscopic properties of mineral dust aerosol. *Geophys. Res. Lett.* 36, L24804.
- Lerach, D. G., 2012. Simulating Southwestern U.S. desert dust influences on severe, tornadic storms. PhD dissertation, Department of Atmospheric Sciences, Colorado State University, pp. 353.
- Lerach, D. G., Cotton, W. R., 2012. Comparing Aerosol and Low-Level Moisture Influences on Supercell Tornadogenesis: Three-Dimensional Idealized Simulations. *American Met. Socy.* 69, 3.
- Levi, Y., Rosenfeld, D., 1996. Ice nuclei, rainwater chemical composition and static cloud seeding effects in Israel. *J. Applied Meteorol.* 35, 1496-1501
- Levin, Z., Ganor, E., Gladstein, V., 1996. The effects of desert particles coated with sulfate on rain formation in the eastern mediterranean. *J. App. Meteor.*, 35, 1511-1523.
- Liao H., Henze, D. K., Seinfeld, J. H., Wu, S., Mickley, L. J., 2007. Biogenic secondary organic aerosol over the United States: Comparison of climatological simulations with observations. *J. Geophys. Res.* 112, D06201, doi:10.1029/2006JD007813.
- Martcorena, B., Bergametti, G., 1995. Modeling the atmospheric dust cycle : 1-design of a soil derived dust production scheme. *J. Geophys. Res.* 100, 16,415–16,430.
- Mellor, G. L., Yamada, T., 1974. A Hierarchy of Turbulence Closure Models for Planetary Boundary Layers. *J. Atmos. Sc.* 31, 1791-1806.
- Mesinger, F., et al., 2006. North American regional reanalysis. *Bull. Am. Meteorol. Soc.*, 87, 343–360.

- Meyers, M. P., Walko, R. L., Harrington, J., Cotton, W. R., 1997. RAMS cloud microphysics parameterization. Part II: The two-moment scheme. *Atmos. Res.* 45, 3-39.
- Petters, M. D., Prenni, A. J., Kreidenweis, S. M., DeMott, P. J., 2007. On measuring the critical diameter of cloud condensation nuclei using mobility selected aerosol. *Aerosol Sci. Technol.* 41(10), 907-913.
- Prospero, J. M., 1999. Long-term measurements of the transport of African mineral dust to the southeastern United States: Implications for regional air quality. *J. Geophys. Res.*, 104, 15917–15927.
- Roberts, P., Hallett, J., 1968. A Laboratory Study Of Ice Nucleating Properties Of Some Mineral Particulates. *Quarterly Journal Of The Royal Meteorological Society*, 94(399).
- Rosenfeld, D., Rudich, Y., Lahav, R. 2001. Desert dust suppressing precipitation: A possible desertification feedback loop. *Proceedings of the National Academy of Sciences*, 98, 5975-5980.
- Saleeby, S. M., Cotton, W. R., 2004. A large droplet mode and prognostic number concentration of cloud droplets in the Colorado State University Regional Atmospheric Modeling System (RAMS). Part I: Module descriptions and supercell test simulations. *J. Appl. Meteor.* 43, 182-195.
- Saleeby, S. M., Cotton, W. R., 2005. A large droplet mode and prognostic number concentration of cloud droplets in the Colorado State University Regional Atmospheric Modeling System (RAMS). Part II: Sensitivity to a Colorado winter snowfall event. *J. Appl. Meteor.* 44, 1912-1929.
- Saleeby, S. M., Cotton, W. R., 2008. A binned approach to cloud-droplet riming implemented in a bulk microphysics model. *J. Appl. Meteorol.* 47, doi:10.1175/2007JAMC1664.1.
- Saleeby, S. M., Borys, R. D., Wetzel, M. A., Simeral, D., Meyers, M. P., Cotton, W. R., McAnelly, R., Larson, N., Heffernan, E., 2006. Model aerosol sensitivity studies and microphysical interactions in an orographic snowfall event. Preprints, 12th Conference on Mountain Meteorology, Santa Fe, NM, Amer. Meteor. Soc.
- Saleeby, S. M., Cotton, W. R., Borys, R. D., Lowenthal, D., Wetzel, M. A., 2007. Relative impacts of orographic forcing and pollution aerosols on mountain snowfall. Preprints, 12th Conference on Mesoscale Processes, Waterville Valley, NH, Amer. Meteor. Soc.
- Saleeby, S. M., Cotton, W. R., Lowenthal, D., 2011. Impact of aerosols on the microphysical processes with an orographic cloud environment. AMS Annual Meeting, Seattle, WA.
- Saleeby, S. M., Cotton, W. R., Lowenthal, D., Borys, R.D., Wetzel, M.A., 2009. Influence of cloud condensation nuclei on orographic snowfall. *J. Appl. Meteor. & Clim.*, 48, 903-922.
- Saleeby, S. M., Berg, S. C. W., van den Heever, S. C., Lecuyer, T., 2010. Impact of cloud-nucleating aerosols in cloud-resolving model simulations of warm-rain precipitation in the East China Sea. *J. Atmos. Sci.*, 67, 3916-3930.
- Sassen, K., DeMott, P., Prospero, J., Poellot, M., 2003. Saharan dust storms and indirect aerosol effects on clouds: Crystal-face results. *Geophys. Res. Lett.* 30, 12, 1633, doi:10.1029/2003GL017371.
- Schaefer, M. B., 1954. Some aspects of the dynamics of populations, important for the management of the commercial marine fisheries. *Inter. Am. Trop. Tuna Comm. Bull.* 1, 27-56.

Schaefer, V. J., 1949. The formation of ice crystals in the laboratory and the atmosphere. *Chem. Rev.*, 44, 291-320.

Smagorinsky, J., 1963. General circulation experiments with the primitive equations, i. the basic experiment. *Monthly Weather Rev.*, 91, 99-164.

Smith, J. D. T., et al. 2007, *ApJ*, 656, 770.

Stokowski, D. M., 2005. The addition of the direct radiative effect of atmospheric aerosols into the regional atmospheric modeling system (RAMS). Master's thesis, Colorado State University, Department of Atmospheric Science, Fort Collins, CO

Tegen, I., Fung, I., 1994. Modeling of mineral dust in the atmosphere: Sources, transport and optical thickness. *J. Geoph. Res.* 99, 22897-22914.

Twohy, C. H., Poellot, M. R., 2005. Chemical characteristics of ice residual nuclei in anvil cirrus clouds: evidence for homogeneous and heterogeneous ice formation. *Atmos. Chem. and Physics*, 5, 2289-2297.

Twohy, C. H., Kreidenweis, S. M., Eidhammer, T., Browell, E. V., Heymsfield, A. J., Bansemer, A.R., Anderson, B. E., Chen, G., Ismail, S., DeMott, P. J., Van Den Heever, S. C., 2009. Saharan dust particles nucleate droplets in eastern Atlantic clouds. *Geophys. Res. Lett.*, 36, L01807, doi:10.1029/2008GL035846.

Twomey, S., 1974. Pollution and the planetary albedo. *Atmos. Environ.* 8, 1251-1256.

Twomey, S., 1977. The influence of pollution on the shortwave albedo of clouds. *J. Atmos. Sci.*, 34, 1149-1152.

Van den Heever, S. C., Carrio, G. G., Cotton, W. R., DeMott, P. J., 2006. Impacts of nucleating aerosol on Florida storms. Part I: Mesoscale simulations. *J. Atmos. Sci.*, 63, 1752-1775.

Walko, R. L., Band, L. E., Baron, J., Kittel, T. G. F., Lammers, R., Lee, T. J., Ojima, D., Pielke, R. A., Taylor, C., Tague, C., Tremback, C. J., Vidale, P. L., 2000. Coupled atmosphere-biophysics-hydrology models for environmental modeling. *J. Appl. Meteor.*, 39, 931-944.

Wang, J., Christopher, S. A., Nair, U. S., Reid, J. S., Prins, E. M., Szykman, J., Hand, J. L., 2006. Mesoscale modeling of Central American smoke transport to the United States: 1. top-down assessment of emission strength and diurnal variation impacts. *J. Geoph. Res.*, 111.

Ward, D. S., Cotton, W. R., 2010. Cold band transition season cloud condensation nuclei measurements in western Colorado. *Atmos. Chem. Phys. Discuss.* 10, C11358-C11361.

Wetzel, M. A., et al., 2004. Mesoscale snowfall prediction and verification in mountainous terrain. *Wea. Forecasting*, 19, 806-828.

Zuberi, B., Bertram, A., Cassa, C., Molina, L., Molina, M., 2002. Heterogeneous nucleation of ice in (NH₄)₂SO₄-H₂O particles with mineral dust immersions. *Geophys. Res. Lett.*, 29, 1504

CHAPTER 3

A study on the impact of dust and aerosol pollution on wintertime orographic precipitation in the Colorado River Basin: Part II Sensitivity Studies

3.1.0 Introduction

This is the second part of a numerical modeling study using RAMS examining the impacts of varying aerosol pollution and dust on precipitation in the Colorado River Basin (CRB). In Part I (Jha et al., 2016) we examined the combined effect of dust and aerosol pollution on the orographic precipitation in the CRB for the winter year 2004-2005.

3.2.0 Summary of Part I

In Part I, we found that in winter season long simulations, dust primarily acts as IN and increases precipitation over an orographic barrier but the combined response of dust and pollution aerosols is dominated by the CCN effects of pollution aerosols which reduced precipitation.

In this chapter (Part II) we perform sensitivity experiments to study the microphysics of the orographic cloud and their response to varying dust in different cloud base heights (cloud base temperatures) regimes. Dust acting as CCN or IN tends to have contrasting impacts when varied in a wet or dry system.

3.2.1 Methods

The setup of RAMS is described in Chapter 2 (Part I). In this paper a series of sensitivity experiments are described to better understand factors influencing the results discussed in Part I.

3.2.2 Experimental methodology

All the winter-season long simulations in Part I were run for 10 day-long periods, which were then cumulated to obtain the winter season, long results. In this chapter we examine specific 10-day periods and perform sensitivity studies to better understand the results in Part I. In these sensitivity studies, dust concentration was multiplied three times and ten times respectively in both the RAMS source dust and the GEOS-Chem ingested dust. As summarized in Table 3.1, sensitivity experiments included a base study which has all dust sources are turned OFF, and only the GEOS-Chem estimated anthropogenic hygroscopic aerosol sources turned ON. Experiment # 2 has both the dust and aerosol pollution data ON. Case 3 has the aerosol sources ON with dust multiplied by a factor of 3. Experiment # 4 has the aerosol sources ON with dust multiplied by a factor of 10. Experiment # 5 and Experiment # 6 are the simulations where dust can act only as CCN and only as IN, respectively.

Table 3.1: Sensitivity Tests Types

Expt 1	Expt 2	Expt 3	Expt 4	Expt 5	Expt 6
a1d0	a1d1	a1d3	a1d10	a1din	a1dccn
AerosolX1	AerosolX1	AerosolX1	AerosolX1	AerosolX1	AerosolX1
Dust OFF	DustX1 Anthropogenic	DustX3	DustX10	Dust can act only as IN	Dust can act only as CCN

Dust and hygroscopic aerosol data were initialized from the GEOS-Chem model and regional dust sources in RAMS. The GEOS-Chem data represents long range transport while dust sources in RAMS represents local sources. These sensitivity experiments are only performed for the RAMS Setup 2 (see Part I) using adsorption theory, updated look-up tables,

and the DeMott (2014) IN nucleation scheme. As described in Part I, GEOS-Chem is used to estimate non-anthropogenic and anthropogenic pollution contributions to CCN concentrations.

3.3.0 Results and discussion

3.3.1 Case Study 1

The Case Study 1 was chosen to see the impact of changing dust on a wet system. During this period cloud bases were lower than Case Study 2 and higher than Case Study 1. Hence it is hypothesized that ice-phase precipitation can be enhanced for low cloud base height clouds by increasing dust acting as IN. In this first case study, the model was run for a period of 10 days, starting on October 22nd. The different cases that were run for the same time period are as follows: a) hygroscopic aerosol ON and dust off (a1d0) b) hygroscopic aerosol ON and dust ON (a1d1), both dust and hygroscopic aerosol are from anthropogenic sources and the RAMS regional dust sources were also turned on, c) hygroscopic aerosol ON and dust multiplied 3 times (a1d3), d) hygroscopic aerosol ON and dust multiplied 10 times (a1d10) e) dust was allowed only to act as CCN (a1dccn) and f) dust was allowed to act as IN (a1din).

It was found that the precipitation increased as the amount of dust in the model was increased from a1d0 to a1d1 to a1d3 to a1d10 during this case study period. Figure 3.1 shows the dust concentration for the three different cases (a1d1, a1d3, a1d10 respectively). The concentration of dust is varied between $(10-70)/\text{cm}^3$ for a1d1 (Figure 3.1a). In the a1d3 dust concentration varies between $(10-270)/\text{cm}^3$ (Figure 3.1b). In the a1d10 runs the dust concentration ranges between $(10-700)/\text{cm}^3$ (Figure 3.1c). The background pollution aerosol concentration is at values predicted by GEOS-Chem and so varies in space and time for all the cases. It can be seen that dust acting as CCN tends to decrease precipitation and dust acting as IN tends to increase precipitation (Figure 3.2). Figure 3.3 show that there are more aggregates in the

a1d10 than a1d3 and a1d1 has the least aggregates. Dust acting as IN leads to the formation of more ice particles; hence it increases the aggregate formation, which roughly varies with the square of ice particle concentrations. The temperature profile indicates higher temperature of the cloud base for this system relative to the Case Study 2 and 3 (Figure 3.4). This is a wet system during this period with more precipitable water available (Figure 3.5). The 500 mb geopotential height fields indicate a trough moving through the period with light zonal winds (Figure 3.6). Figure 3.7 shows the topography of the Grid 3 with the location of the upper San Juan site in the map with latitude 37.29 degrees and longitude -106.50 degrees. Figure 3.8 shows the comparison of model data with the Snotel observation data at the upper San Juan site and RAMS simulated precipitation mostly stays in agreement with the observation data.

3.3.2 Case Study 2

In the second case study, the model was run for a period of 10 days, starting on March 31st 2005 and ending on April 10th 2005. This was a period with higher cloud base heights and less moist than Case Study 1. The model was run with a) aerosol ON and dust OFF (a1d0) b) aerosol ON and dust ON (a1d1), both dust and aerosol are from anthropogenic sources and the RAMS regional dust sources were also turned on, c) aerosol ON and dust multiplied 3 times (a1d3), d) aerosol ON and dust multiplied 10 times (a1d10). The dust concentration profile is displayed in Figure 3.9: a, b, c for the three dust ratios respectively and the background pollution aerosol concentration (Figure 3.10)

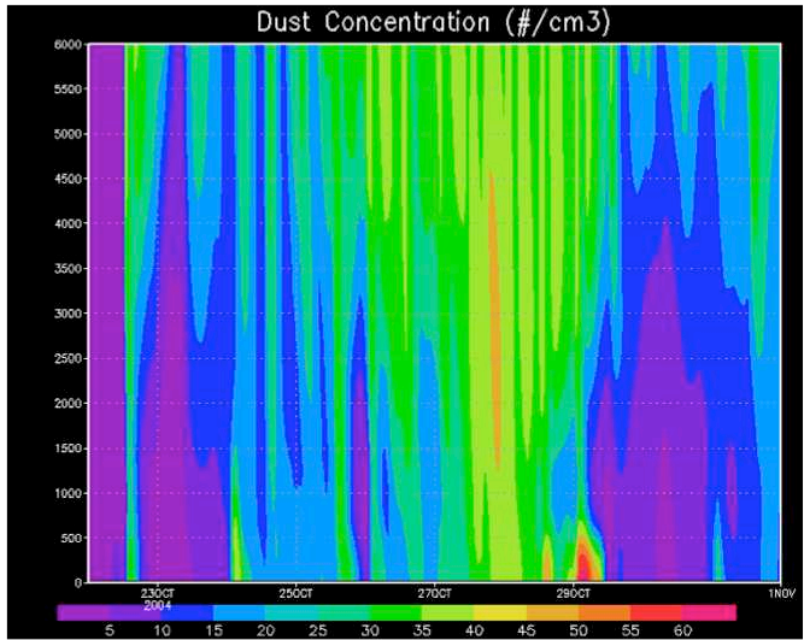


Figure 3.1a: Dust concentration profile for a1d1 for Case Study 1

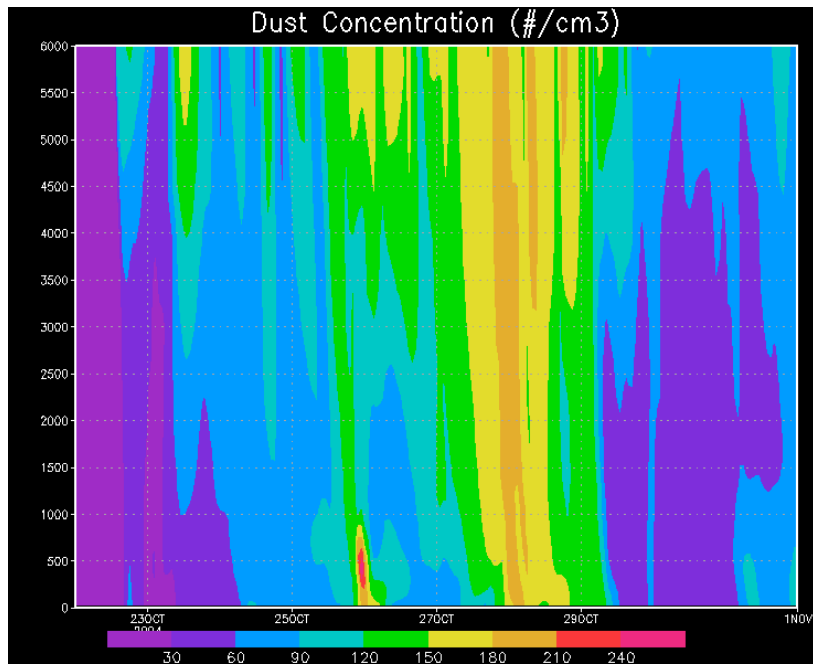


Figure 3.1b: Dust concentration profile for a1d3 for Case Study 1

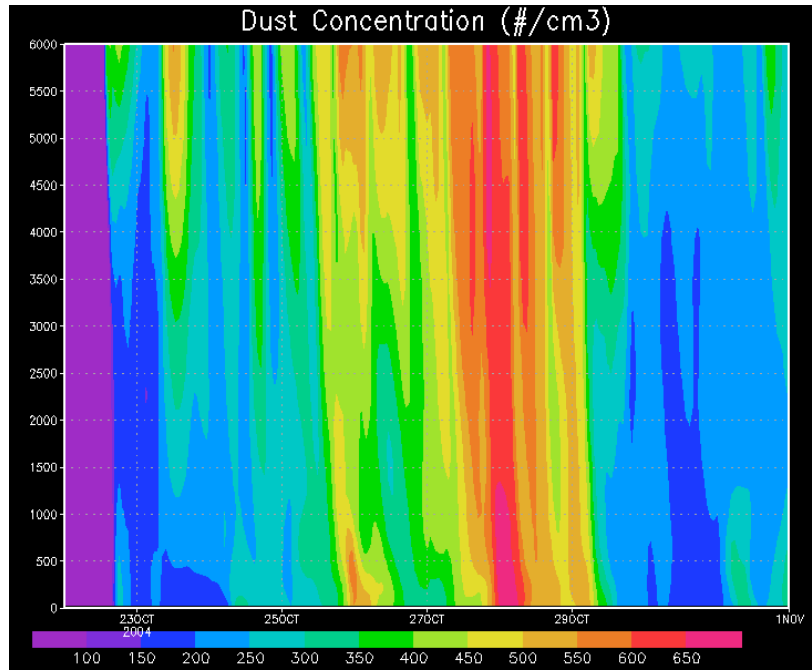


Figure 3.1c: Dust concentration profile for a1d10 for Case Study 1

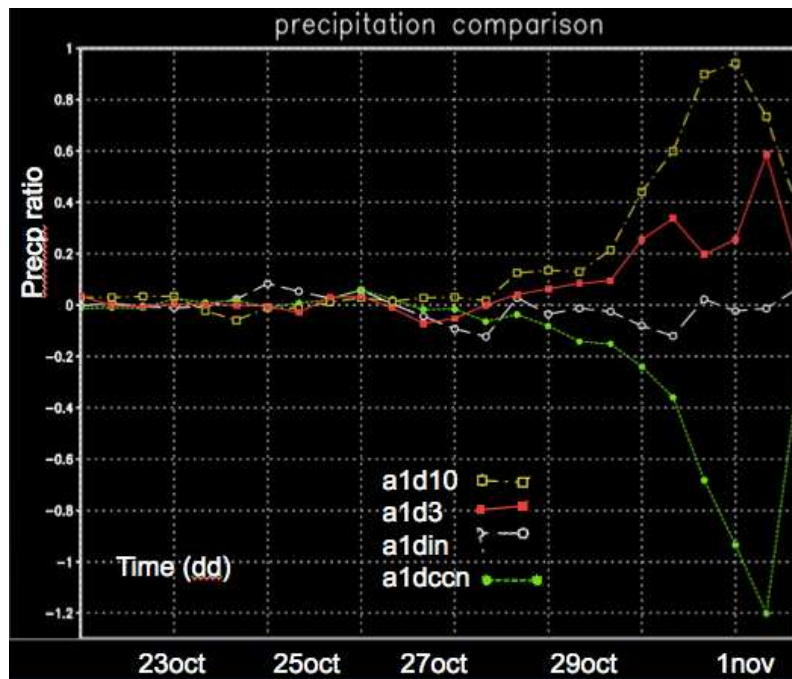


Figure 3.2: Plot of precipitation with no dust compared to a1d3, a1d10, a1dccn, a1din

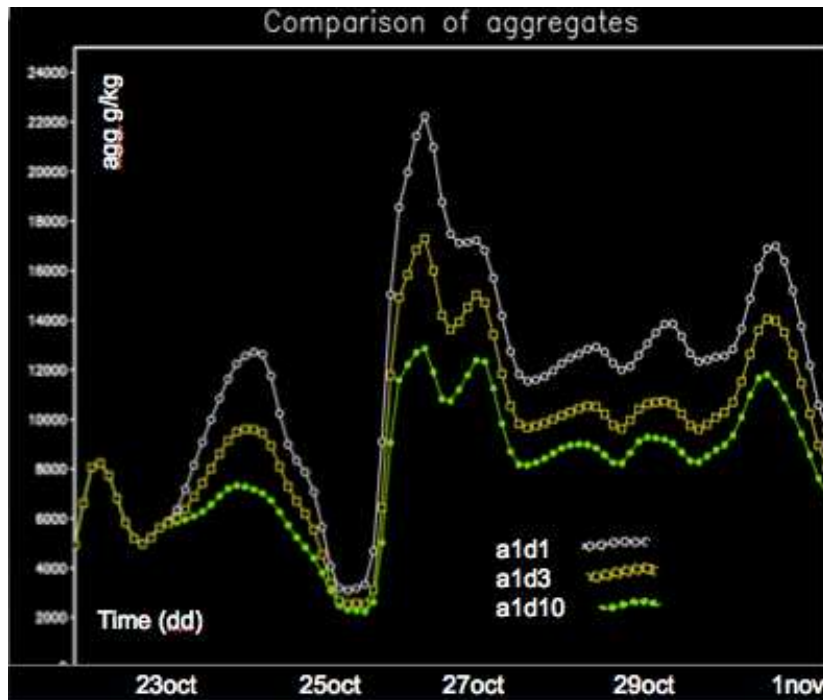


Figure 3.3: Plot of aggregates for the different cases

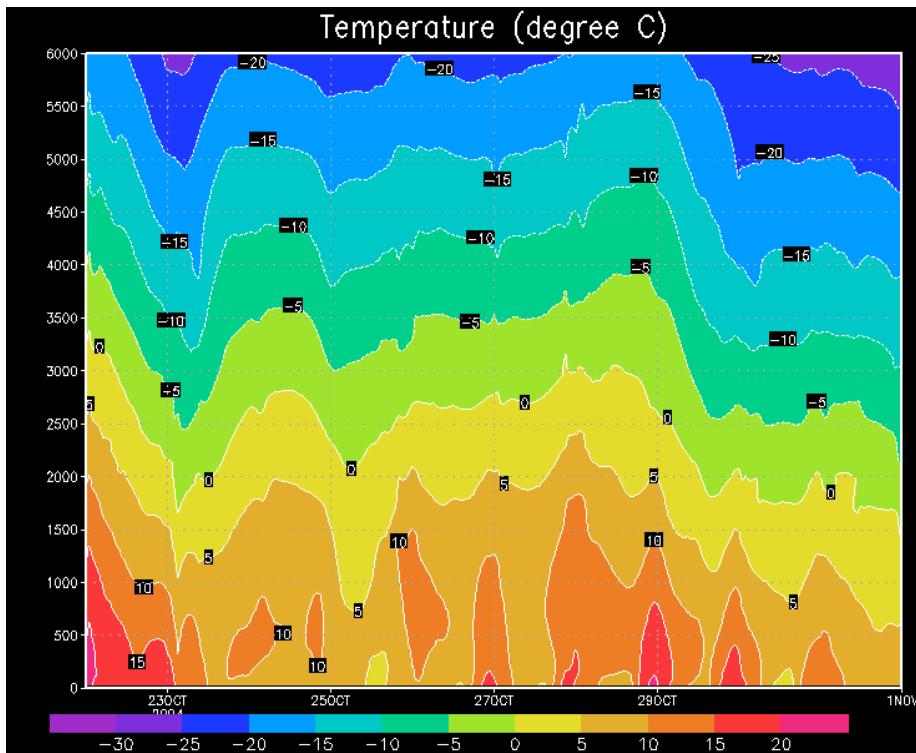


Figure 3.4: Temperature profile of study for the Case Study 1

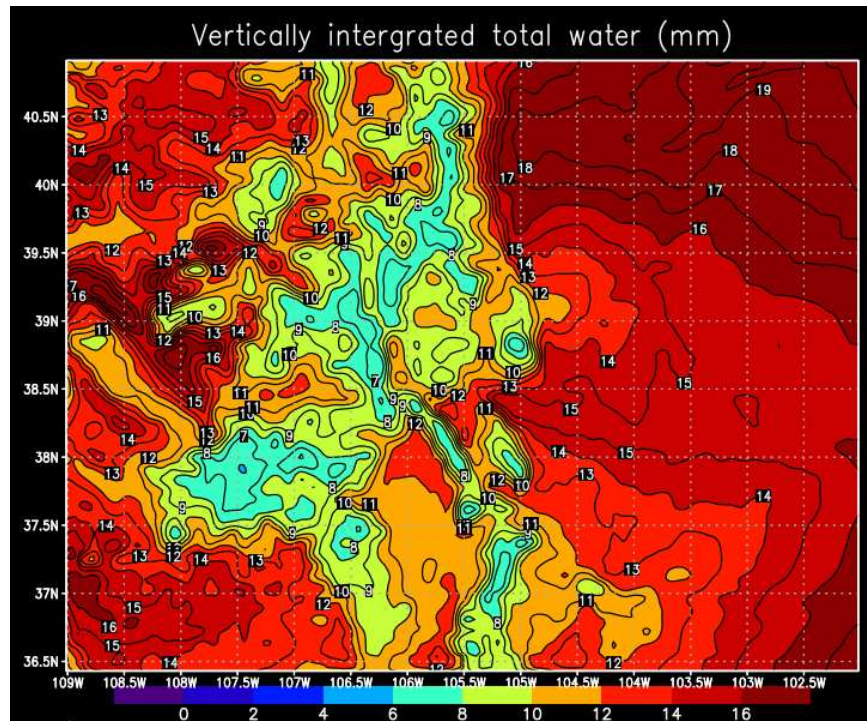


Figure 3.5: Total precipitable water for grid 3 for the Case Study 1

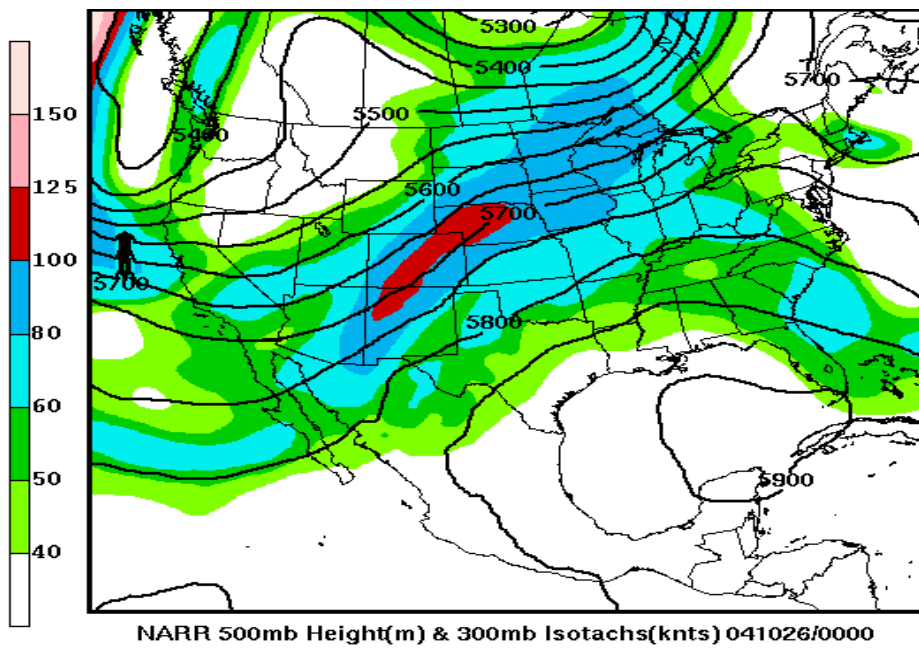


Figure 3.6: 500 mb geopotential heights for the Case Study 1

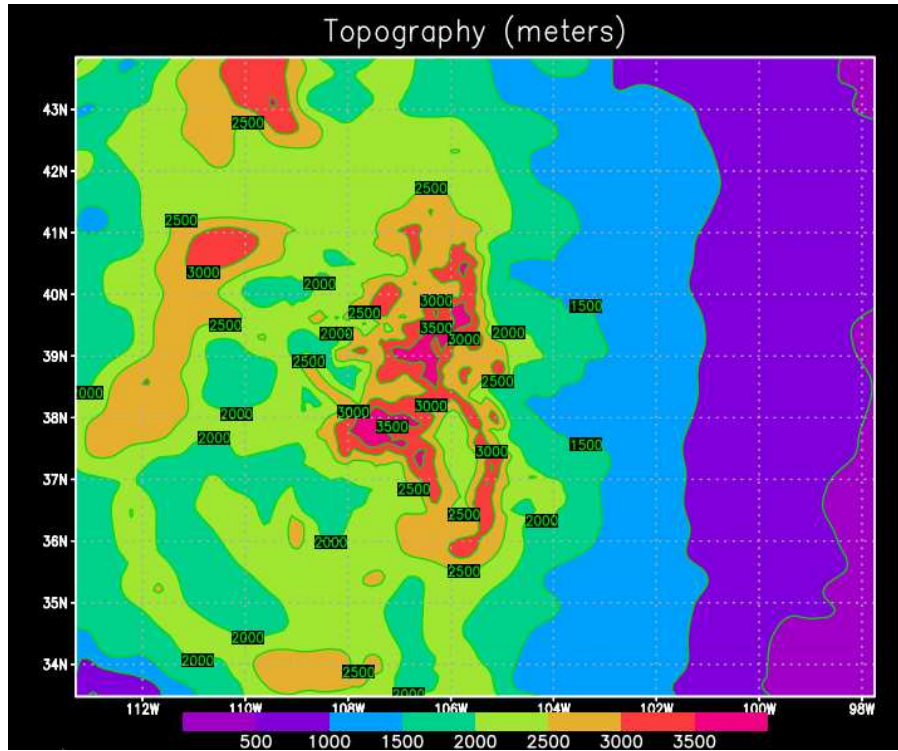


Figure 3.7: Topography of Grid 3 of the area of study for the Case Studies

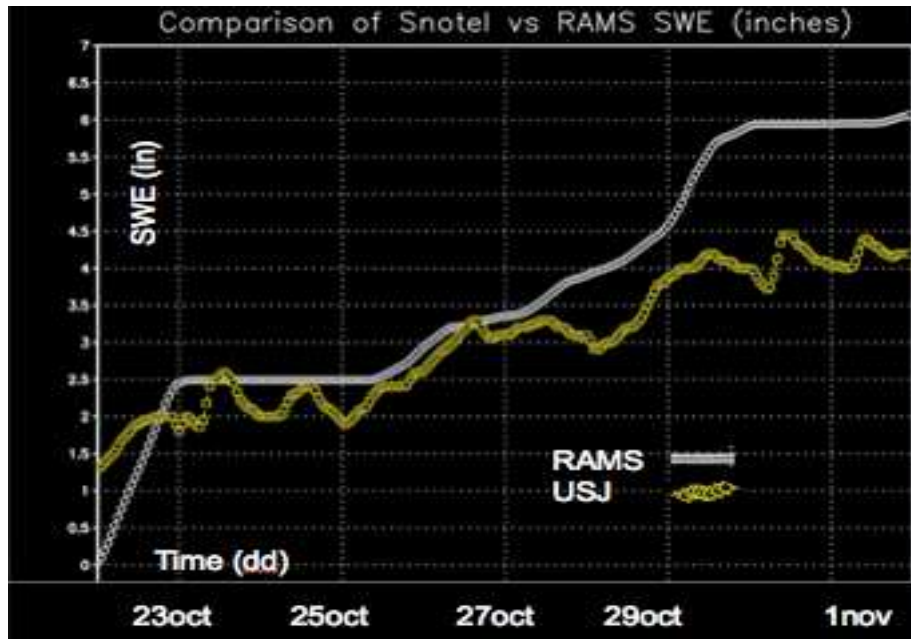


Figure 3.8: Plot for comparison of Snotel and RAMS snow water equivalent in inches

varies in space and time in accordance to the GEOS-Chem estimates including anthropogenic sources for all the cases. Figure 3.11 shows the ratio of precipitation for a) a1d1 b) a1d3 and c) a1d10 with respect to the case when dust was OFF. It was found that precipitation starts decreasing after adding dust to the system at around April 6th. The model was run with dust acting as only CCN and IN and the precipitation for those two cases was again compared to the NO dust case. It was found that dust acting solely as IN was the case that yields the least precipitation (Figure 3.12). The temperature profile of this case was also plotted and it was found that the cloud bases were colder as compared to Case Study 1 (Figure 3.13). The precipitable water available for the system was lower than that for the CASE study 1(Figure 3.14). A major difference between this and Case 1, was the very high zonal southwesterly wind right at the period when the transition happened (Figure 3.15).

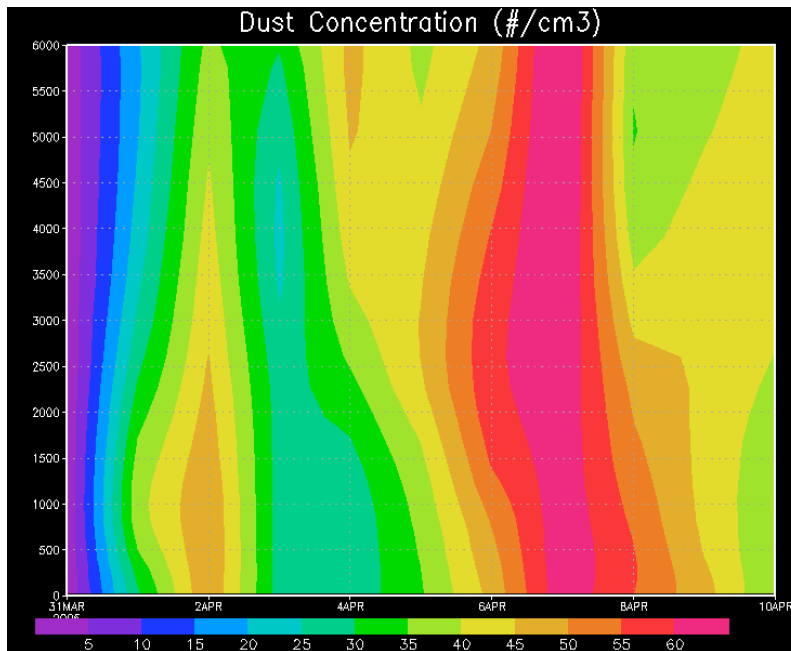


Figure 3.9a: Dust concentration profile for a1d1 for Case Study 2

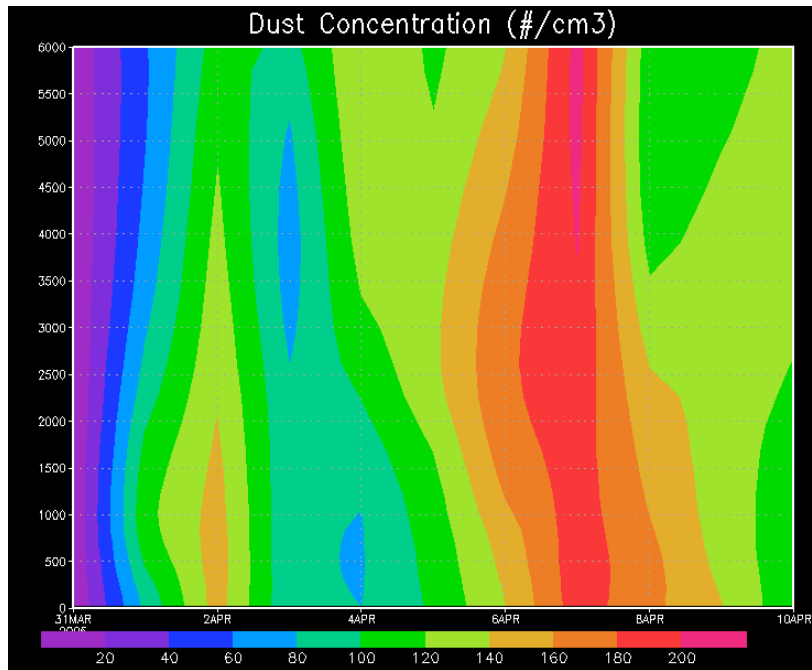


Figure 3.9b: Dust concentration profile for a1d3 for Case Study 2

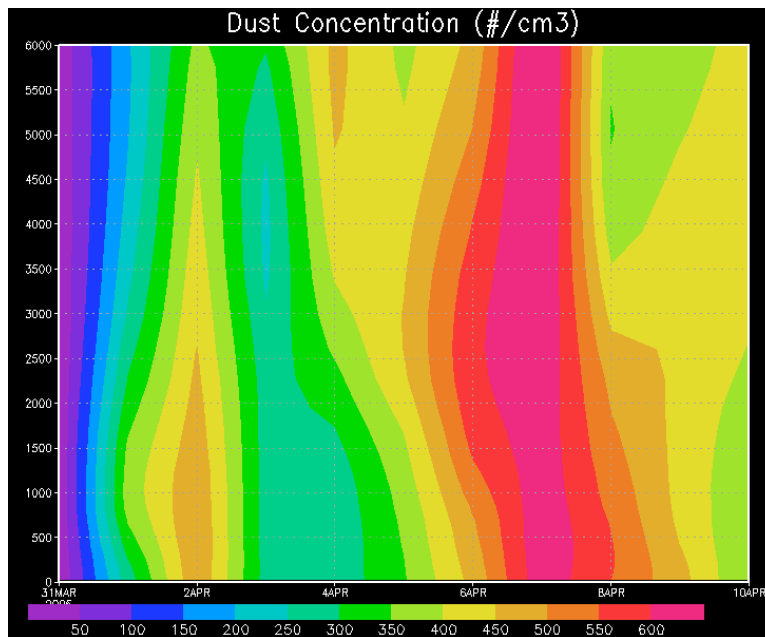


Figure 3.9c: Dust concentration profile for a1d10 for Case Study 2

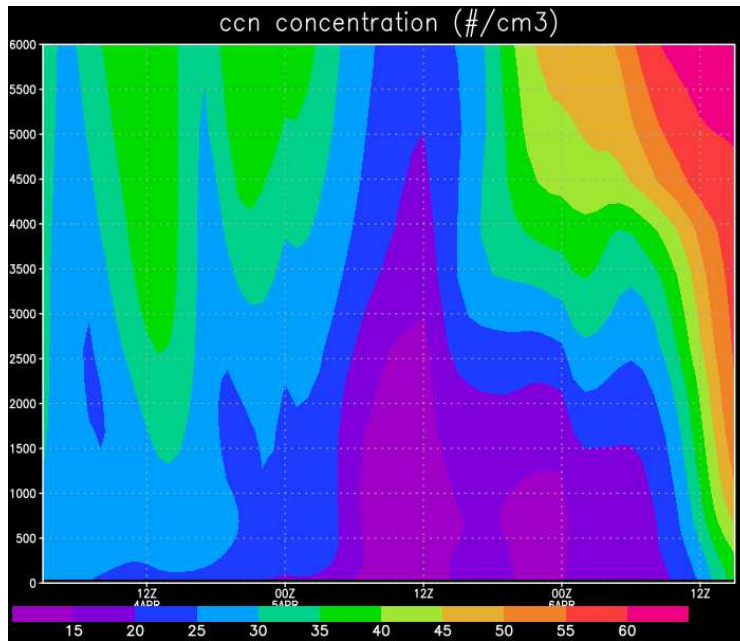


Figure 3.10: Potential CCN concentration profile for Case Study 2

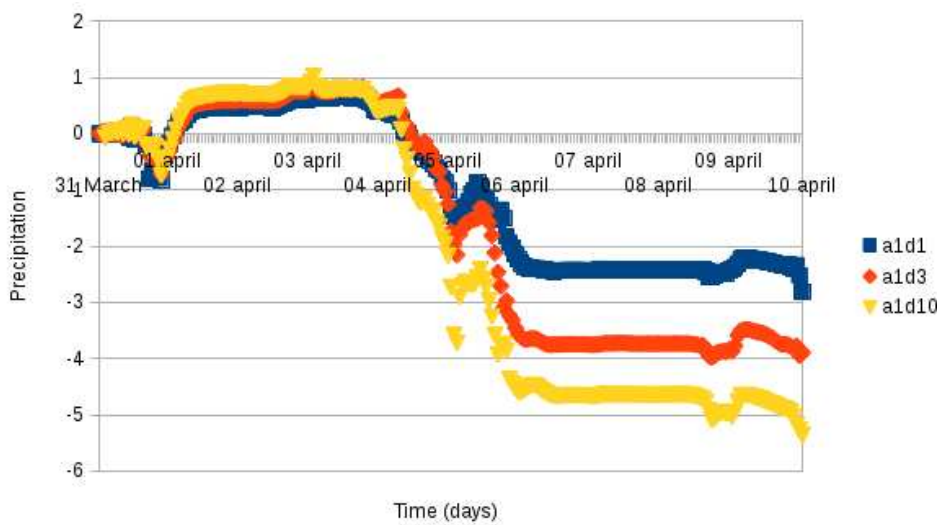


Figure 3.11: Plot of precipitation with no dust compared to a1d1, a1d3, a1d10

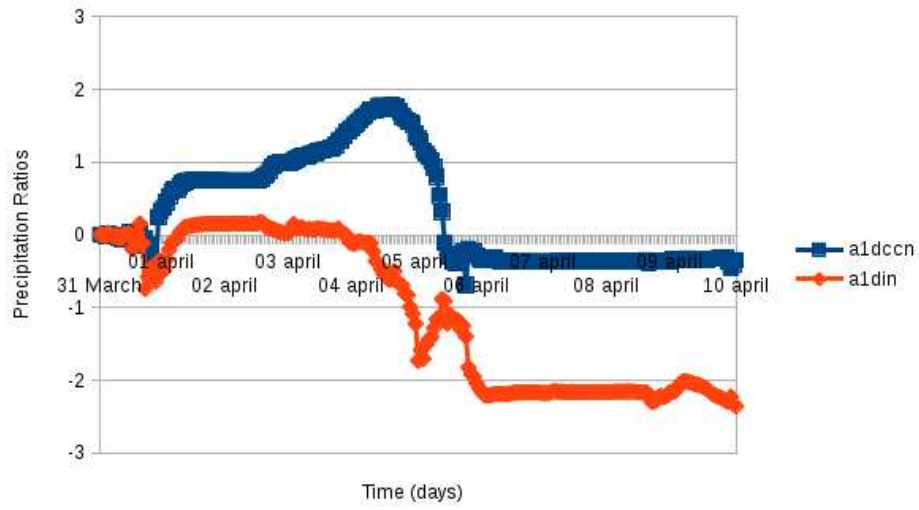


Figure 3.12: Plot of precipitation with no dust compared to a1dccn and a1din

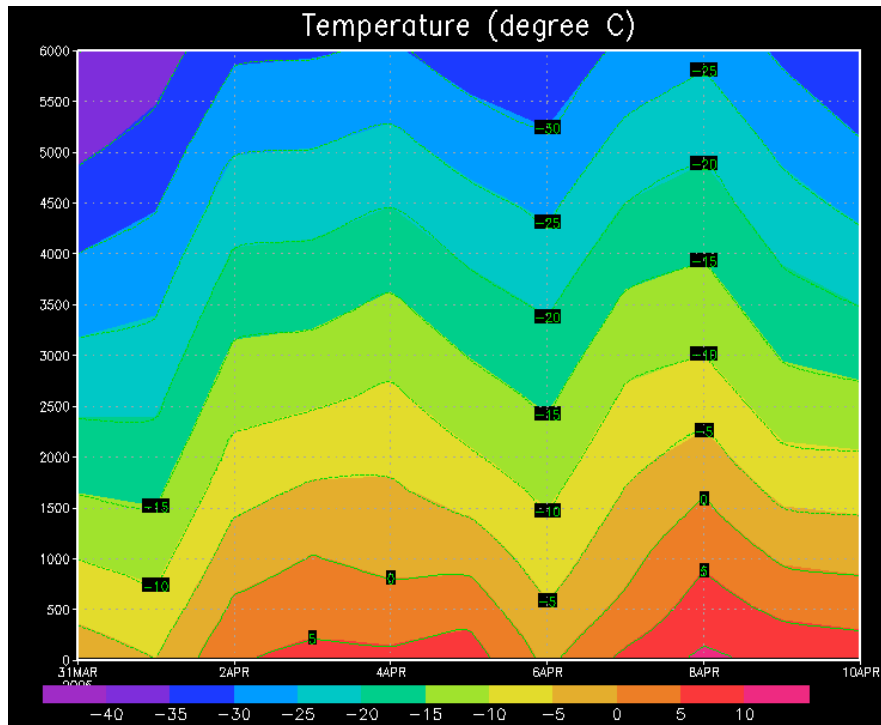


Figure 3.13: Temperature profile of study for the Case Study 2

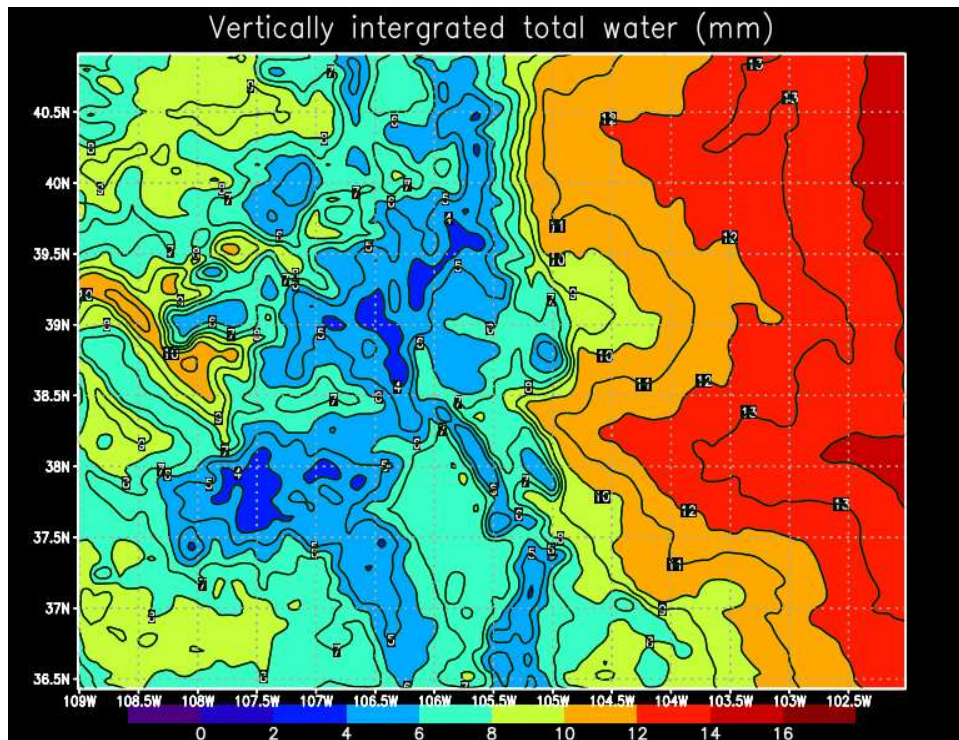


Figure 3.14: Total precipitable water for grid 3 for the Case Study 2

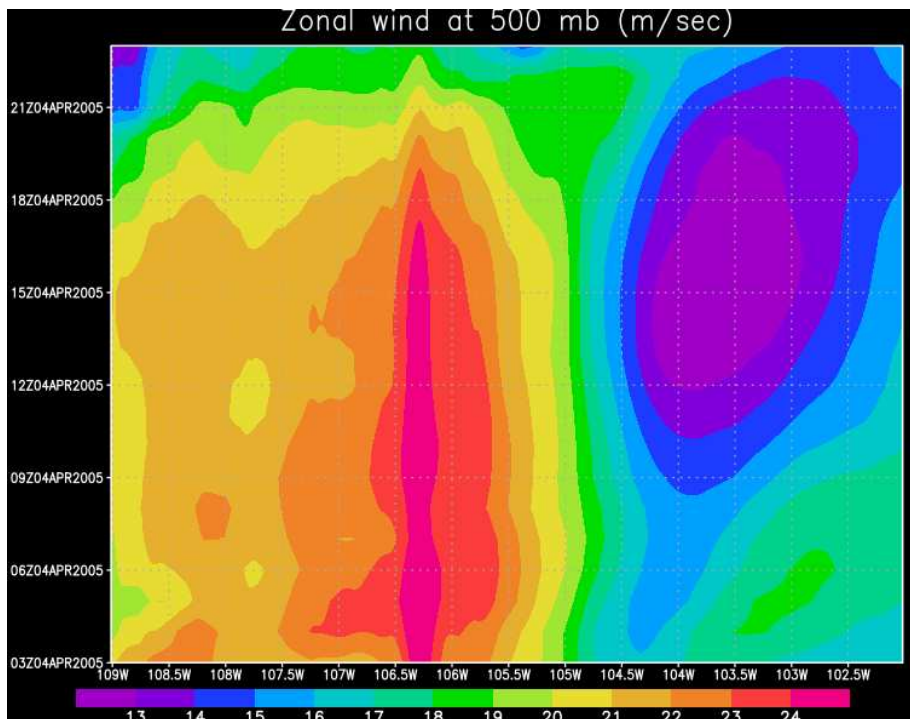


Figure 3.15: 500 mb zonal wind speed for the Case Study 2

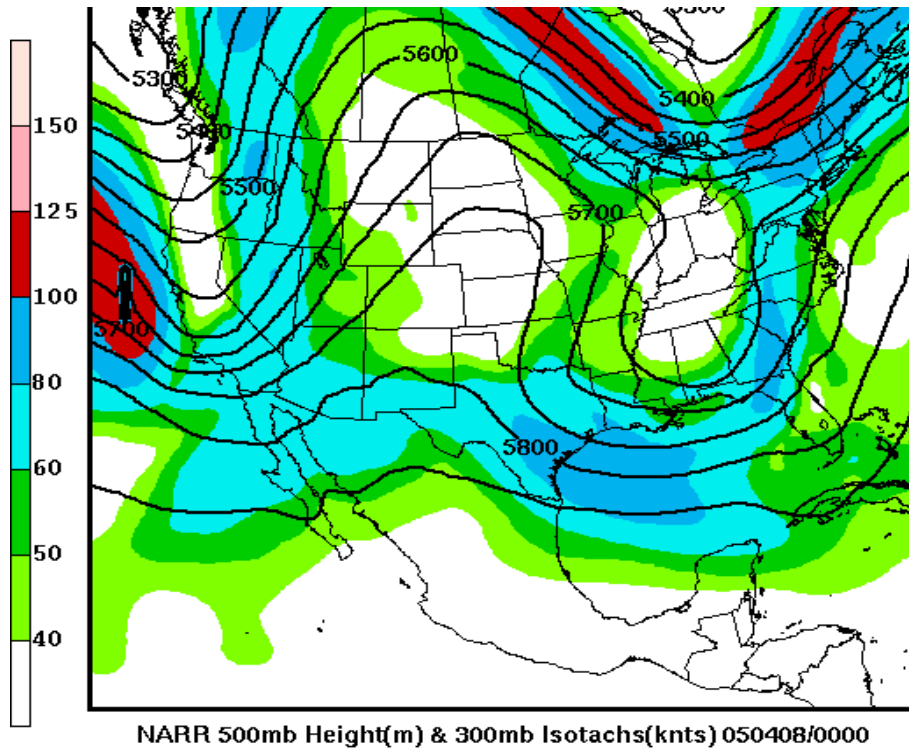


Figure 3.16: 500-hPa geopotential height (m) from the NARR dataset for Case Study 2

The strong wind contributes to precipitation drifting into the subsiding region and hence decreasing it. The 500-hPa geopotential height indicates a ridge passing through the region (Figure 3.16).

3.3.3: Case Study 3

The third study was started on October 2nd and run for duration of 10 days. Dust was varied in different experiments (Figure 3.17) and pollution aerosol varied spacially and temporally according to GEOS-Chem estimates (Figure 3.18) following the pattern in Table 3.2 and precipitation difference was observed for the duration. This was a period with very warm cloud bases temperatures (Figure 3.19) and lower cloud base height with greater availability of moisture and hence it is important to see how changing dust impacts precipitation for the period. When dust was increased 3 times precipitation increased slightly (2.7%) but when dust was

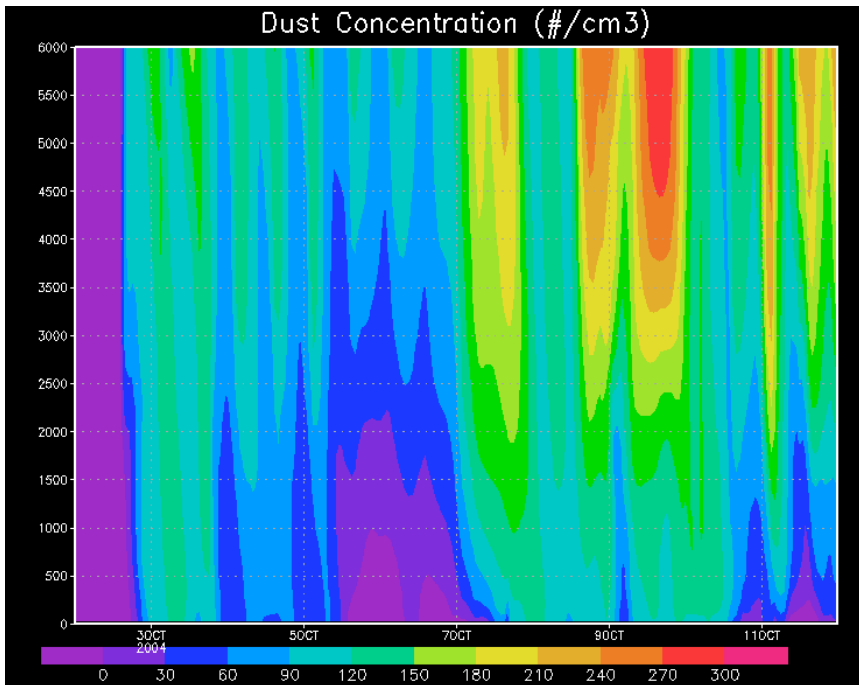


Figure 3.17: Dust concentration profile for a1d1 for Case Study 3

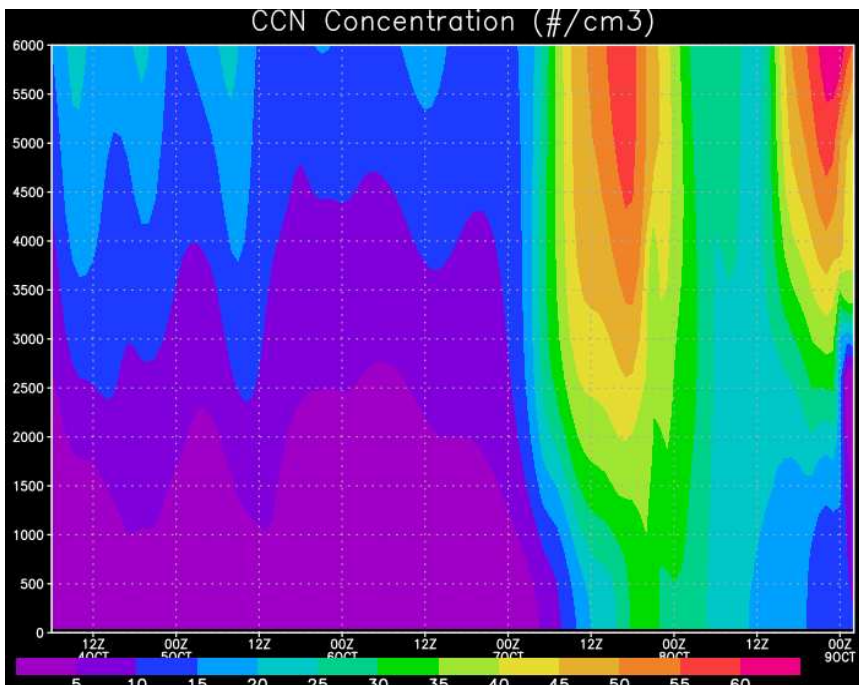


Figure 3.18: CCN concentration profile for the period for Case Study 3

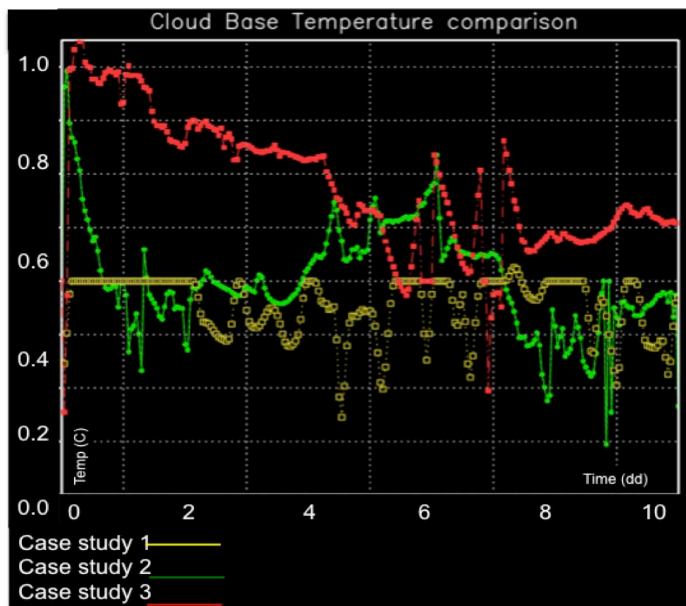


Figure 3.19: Plot of cloud base temperature for the three case studies. Case Study 3 is dominated by lower cloud bases and hence higher cloud base temperatures

increased 10 times precipitation decreased by -16.9% in the CRB (Figure 3.20). When dust is increased 10 times the precipitation in the system is reduced due to over-seeding of IN producing numerous small ice crystals. The temperature profile suggests a warmer cloud base as compared to the Case Study 1. The availability of supercooled liquid water that could be transferred to snow by riming is increased here, which suppressed drizzle formation (Figure 3.21). The figure shows the comparison of the experiments as dust is increased from a1d1-a1d3-a1d10. The total mass of the water in the drizzle category reduces with increasing dust. The curve has been normalized by the maximum value. The system seems to be wetter than Case 2 and the temperature profile suggests warmer cloud bases in this case compared to the system in Case 1 and Case 2 initially (Figure 3.22) The total precipitable water indicated it as a wet period. (Figure 3.23). The colder cloud temperatures seem to prevail towards the later part of the system and the dust as CCN affects were more dominant (Figure 3.24) and therefore, we see non-monotonicity when increasing dust 10 times. Carrio et al., 2014 did an idealized study and varied both CCN concentrations and the low level moisture in the Sierra Nevada mountains in a 2D modeling

RAMS modeling experiment. They observed that for the low level moisture (i.e., cloud with the high cloud bases) increasing CCN decreased the integral mass of snow precipitation. However, for lower cloud bases (higher low level moisture amounts) or cloud with warmer cloud base, they simulated a non-monotonic behavior.

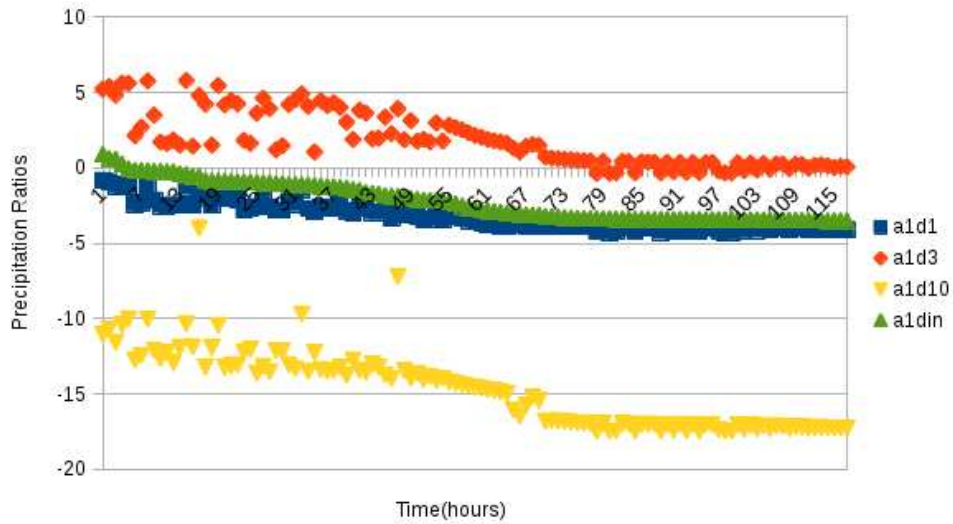


Figure 3.20: Plot of precipitation with no dust compared to a1d1, a1d3, a1d10, a1din

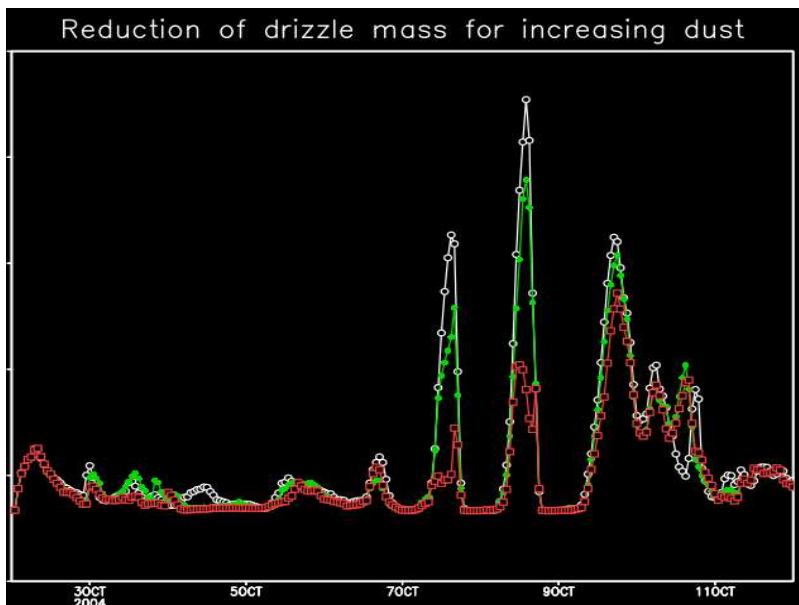


Figure 3.21: Comparison Total mass of water in drizzle category white: a1d1, green: a1d3 and red: a1d10

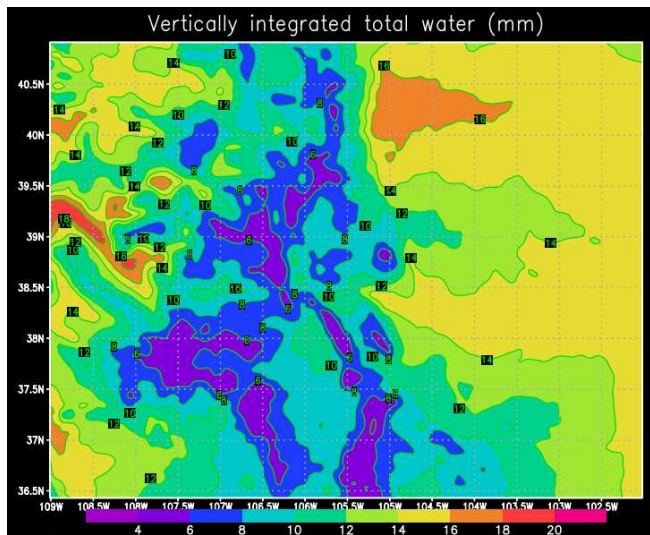


Figure 3.22: Total precipitable water for grid 3 for the Case Study 3

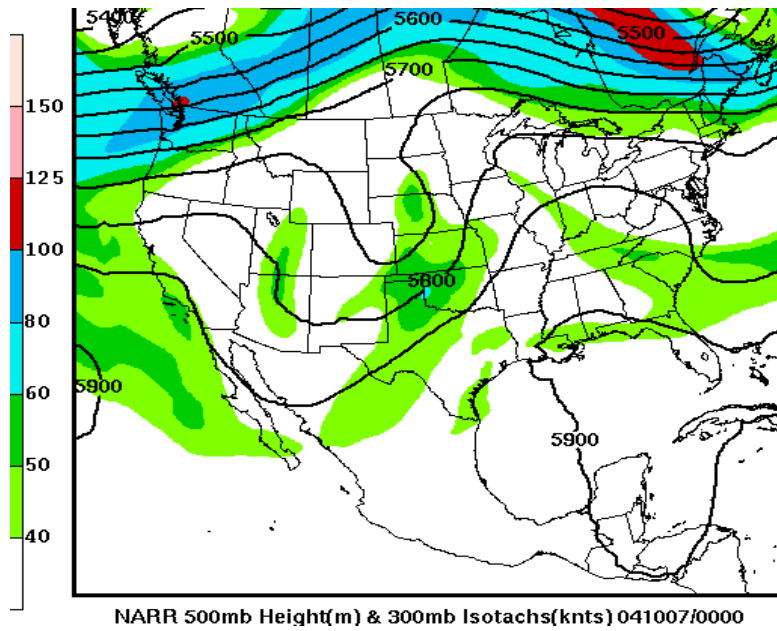


Figure 3.23: 500-hPa geopotential height (m) from the NARR dataset for Case Study 3

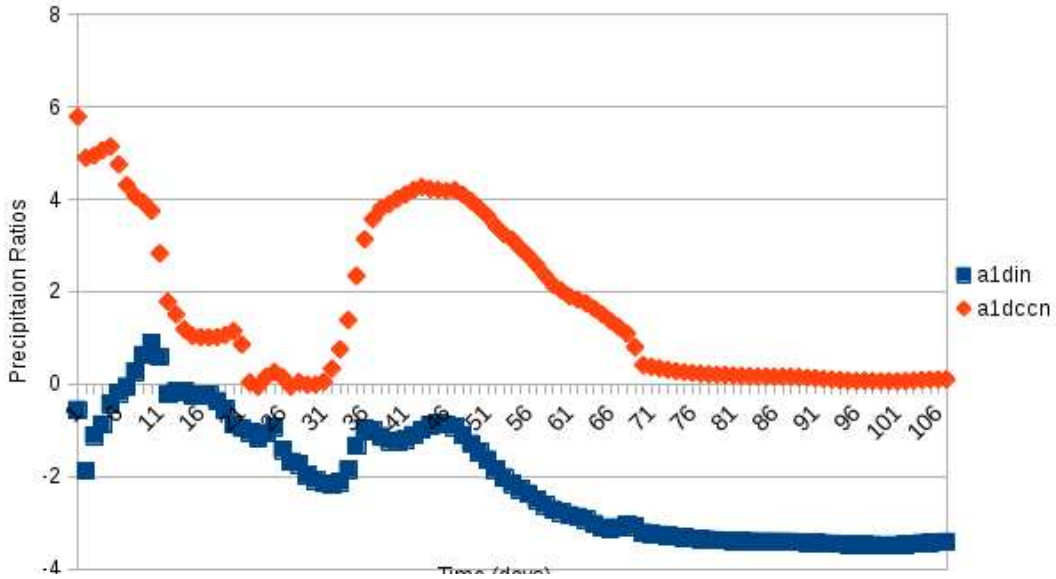


Figure 3.24: Plot of precipitation with no dust compared to dust acting only as IN and CCN

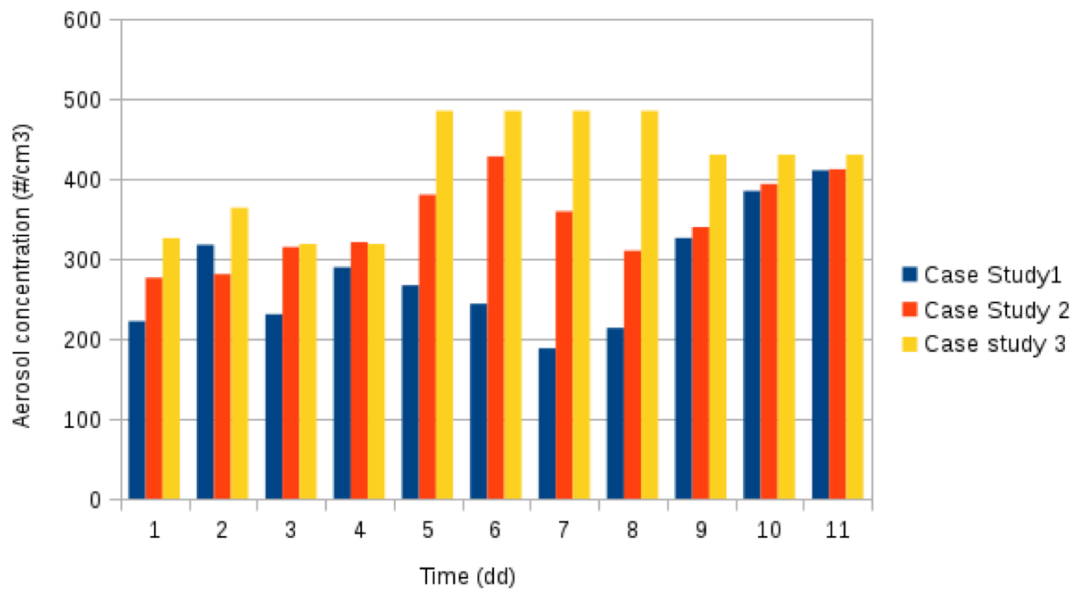


Figure 3.25: Plot of aerosol concentrations for the three case studies. Case Study 3 is the one that has higher concentration of aerosols

In a different test, the model was run to see the change in response in precipitation between anthropogenic and non-anthropogenic sources of dust and pollution aerosol and it was found that anthropogenic or non-anthropogenic sources of dust and aerosol pollution have varying impact on the precipitation. In one case they had similar response. Figure 3.26 shows the total precipitation response when the model was run for the following cases. a) aerosol on and dust on (a1d1), both dust and aerosol are from anthropogenic sources, b) aerosol on and dust on (a1d1), both dust and aerosol are from non- anthropogenic sources case c) aerosol on and dust off (a1d0) d) aerosol on and dust multiplied 3 times e) aerosol on and dust multiplied 10 times a1d10 and It was found that the precipitation was a maximum for the case a1d10 and least for the no dust case (neither anthropogenic nor non-anthropogenic sources). The precipitation for a1d3 was less than the a1d1. However, in yet another case study anthropogenic aerosol had a bigger impact on precipitation (figure not shown here).

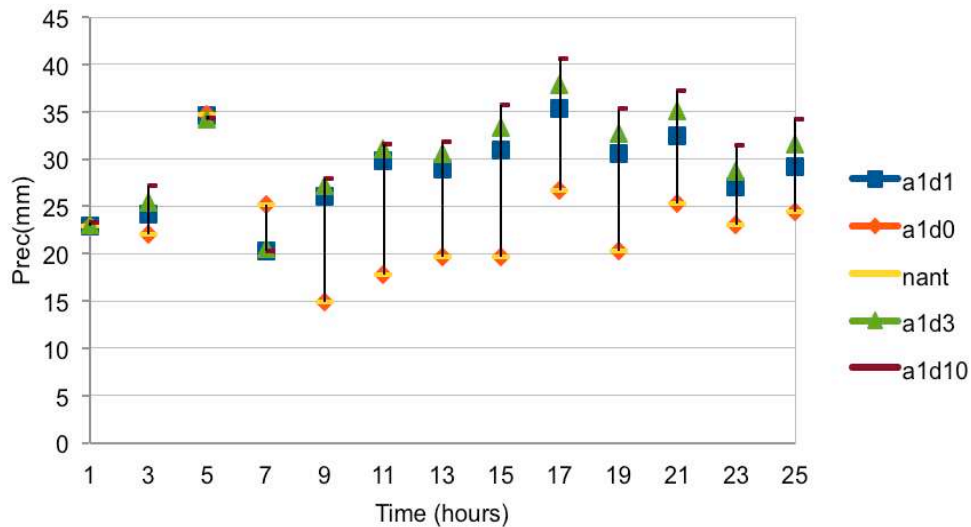


Figure 3.26: Plot of precipitation for a) a1d1 b) a1d0 c) nant d) a1d3 e) a1d10

3.4.0 Conclusion

In three different case studies dust concentration was varied to examine the response on the precipitation in an orographic cloud system. RAMS V 6.0 was used for the sensitivity tests. It was found that adding dust in a wet storm (Case Study 1) results in dust acting as IN to increase precipitation (Table 3.2). This is due to the greater amounts of supercooled liquid water of the system available to enhance precipitation. However, in a dry storm system (Case Study 2), the clouds were overseeded with IN which lead to a decrease in precipitation. It is also evident that the CCN concentration did not play much of a role during the sensitivity runs as it remains low throughout the period of change in precipitation. Dust acts as CCN and hence decreases precipitation after April 6th Case Study 2. Case Study 3 was a period with very warm cloud bases temperatures and lower cloud base height with greater availability of moisture. Dust acting as CCN suppressed drizzle formation and increased SLWC, enhancing riming. The response is not monotonic with dust. The reason is that for moderate dust concentrations, aerosol pollution dominates but owing to warm cloud bases, drizzle formation is active. For higher concentrations of dust, drizzle acting as CCN suppresses warm rain processes, SLWC increases, and ice-phase precipitation is enhanced. For dust enhanced 10X, SLWC is enhanced, but riming is suppressed owing to small droplet sizes, thus ice phase precipitation could not produce as much precipitation

Table 3.2: Results of dust sensitivities in the three Case Studies

	Precipitation Difference (%)	D3-D1	D10-D1
Case Study 1	GRID 3	0.82	2.255
	CRB	0.49	1.290
Case Study 2	GRID 3	-4.57	-5.77
	CRB	-4.63	-5.62
Case Study 3	GRID 3	2.718	-16.907
	CRB	1.642	-15.560

as lesser amounts of dust. Case Study 3 had also the higher concentration of aerosols as seen in Figure 3.25.

For the three case studies, the results of the sensitivity experiments suggests that in Case Study 1, the cloud bases are colder, hence increasing dust increases precipitation as the IN effect is always dominant and there is more aggregates formation. In Case study 3, the cloud bases are warmer (Figure 3.19) hence dust behaves non-monotonically when varied with respect to aerosol pollution. Dust acting, as CCN tends to reduce precipitation over an orographic barrier as there would be less riming formation as amount of dust acting as CCN increases in the system. Dust added to a wet storm in Case Study 1 tends to increase precipitation with the more available precipitable water, while it exhibits opposing affects for a dry system.

Changes in microphysics impacts the precipitation of the system but the dynamical forcings of a storm system which affects wind strength and temperature of the cloud base and water content of the storm has a larger impact on the system. More studies need to be done to analyze the response in different cloud regimes and geographical locations.

REFERENCES

- Barnett, T. P., Pierce, D. W., 2009. Sustainable water deliveries from the Colorado River in a changing climate. *Proc. Natl. Acad. Sci. USA* 106, 7334–7338.
- Bey, I., Jacob, D. J., Yantosca, R. M., Logan, J. A., Field, B. D., Fiore, A. M., Li, Q., Liu, H. Y., Mickley, L. J., Schultz, M. G., 2001. Global modeling of tropospheric chemistry with assimilated meteorology: Model description and evaluation. *J. Geophys. Res.* 106, 23073–23095.
- Borys, R. D., Wetzal, M. A., 1997. Storm Peak Laboratory: A research, teaching and service facility for the atmospheric sciences. *Bull. Amer. Meteor. Soc.* 78, 2115-2123.
- Borys, R. D., Lowenthal, D. H., Mitchell, D. L., 2000. The relationships among cloud microphysics, chemistry, and precipitation rate in cold mountain clouds. *Atmos. Environ.* 34, 2593–2602.
- Borys, R. D., Lowenthal, D. H., Cohn, S. A., Brown, W. O. J., 2003. Mountaintop and radar measurements of anthropogenic aerosol effects on snow growth and snowfall rate. *Geophys. Res. Lett.*, 30, 1538.
- Wainwright, C. D., Pierce, J. R., Liggio, J., Strawbridge, K. B., Macdonald, A. M., Leitch, R. W., 2012. The effect of model spatial resolution on Secondary Organic Aerosol predictions: a case study at Whistler, BC, Canada. *Atmos. Chem. Phys.*, 12, 10911-10923.
- Carrió, G. G., Cotton, W. R., 2014. On the buffering of CCN impacts on wintertime orographic clouds: An idealized examination. *Atmos. Res.* 137, 136-144.
- Christensen, N. S., Lettenmaier, D. P., 2007. A multimodel ensemble approach to assessment of climate change impacts on the hydrology and water resources of the Colorado River Basin. *Hydrol. Earth Sys. Sci.* 11, 1417-1434.
- Cooper, W. A., Bruintjes, R. T., Mather, G. K., 1997. Calculations pertaining to hygroscopic seeding with flares. *J. Appl. Meteor.* Boston, MA, 36, 1449-1469.
- DeMott, P. J., Sassen, K., Poellot, M. R., Baumgardner, D., Rodgers, D. C., Brooks, S. D., Prenni, A. J., Kreidenweis, S. M., 2003. African dust aerosols as atmospheric ice nuclei. *Geophys. Res. Lett.* 30, 1732, doi:10.1029/2003GL017410.
- DeMott, P. J., Petters, M. D., Prenni, A. J., Carrico, C. M., Kreidenweis, S. M., Collett, J. L., Moosmuller, H., 2009. Ice nucleation behavior of biomass combustion particles at cirrus temperatures. *J. Geophys. Res.* 114, D16205, doi: 10.1029/2009jd012036.
- DeMott, P. J., Meyers, M. P., Cotton, W. R., 1994. Parameterization and impact of ice initiation processes relevant to numerical model simulations of cirrus clouds. *J. Atmos. Sci.* 41, 77-90.

- DeMott, P. J., Prenni, A. J., Liu, X., Petters, M. D., Twohy, C. H., Richardson, M. S., Eidhammer, T., Kreidenweis, S. M., Rogers, D. C., 2010. Predicting global atmospheric ice nuclei distributions and their impacts on climate. *P. Natl. Acad. Sci. USA*, 107, 11217–11222.
- DeMott, P. J., Prenni, A. J., McMeeking, G. R., Sullivan, R. C., Petters, M. D., Tobo, Y., Niemand, M., Möhler, O., Snider, J. R., Wang, Z., Kreidenweis, S. M., 2014. Integrating laboratory and field data to quantify the immersion freezing ice nucleation activity of mineral dust particles, *Atmos. Chem. Phys. Discuss.* 14, 17359–17400.
- DeMott, P. J., Cziczo, D. J., Prenni, A. J., Murphy, D. M., Kreidenweis, S. M., Thomson, D. S., Borys, R., Rogers, D. C., 2003. Measurements of the concentration and composition of nuclei for cirrus formation. *P. Natl. Acad. Sci. USA*, 100, 14655-14660.
- Fairlie, T. D., Jacob, D. J., Park, R. J., 2007. The impact of transpacific transport of mineral dust in the United States. *Atmos. Environ.* 41, 1251–1266.
- Gagin, A., 1965. Ice Nuclei, their physical characteristics and possible effect on precipitation initiation: *Proc. Tokyo-Sapporo Int. Conf. On Cloud Physics, Sapporo, Japan, Int. Assoc. of Meteor. and Atmos. Phys. of the IUGG.* 155-162.
- Ginoux, P., Chin, M., Tegen, I., Prospero, J. M., Holben, B., Dubovik, O., Lin, S. J., 2001. Sources and distributions of dust aerosols simulated with the GOCART model, *J. Geophys. Res.* 106, 20255–20274.
- Givati, A., Rosenfeld, D., 2004. Quantifying precipitation suppression due to air pollution. *J. Appl. Meteor.* 43, 1038–1056.
- Givati, A., Rosenfeld, D., 2005. Separation between cloud-seeding and air pollution effects. *J. Appl. Meteor.* 44, 1298–1314.
- Heymsfield, A. J., Sabin, R. M., 1989. Cirrus crystal nucleation by homogeneous freezing of solution droplets. *J. Atmos. Sci.* 46, 2252–2264.
- Hung, H. M., Malinowski, A., Martin, S. T., 2003. Kinetics of heterogeneous ice nucleation on the surfaces of mineral dust cores inserted into aqueous ammonium sulfate particles. *J. Of Phys. Chem.* 107, 1296-1306.
- Isono, K., Komabayasi, M., Ono, A., 1959. Volcanoes as a source of atmospheric ice nuclei. *Nature.* 183, 317-318.
- Jirak, I. L., Cotton, W. R., 2006. Effect of air pollution on precipitation along the Front Range of the Rocky Mountains. *J. Appl. Meteor.* 45, 236–245.
- Kain, J. S., Fritsch, J. M., 1993. Convective parameterization for mesoscale models: The Kain–Fritsch scheme, in: Emanuel, K. A., et al., (eds.), *The Representation of Cumulus Convection in Numerical Models*, *Meteor. Monogr.* 24, Amer. Meteor. Soc., 165–170.

- Klemp, J. B., Wilhelmson, R. B., 1978. Simulations of right and left moving storms produced through storm-splitting. *J. Atmos. Sci.* 35, 1097-1110.
- Koehler K. A., Kreidenweis, S. M., DeMott, P. J., Petters, M. D., Prenni, A. J., Carrico, C. M., 2009. Hygroscopicity and cloud droplet activation of mineral dust aerosol. *Geophys. Res. Lett.*, 36, L08805.
- Kumar, P., Sokolik, I. N., Nenes, A., 2011. Measurements of cloud condensation nuclei activity and droplet activation kinetics of fresh unprocessed regional dust samples and minerals. *Atmos. Chem. Phys.*, 11, 3527–3541.
- Lerach, D. G., Cotton, W. R., 2011. Comparing Aerosol and Low-Level Moisture Influences on Supercell Tornadoogenesis: Three-Dimensional Idealized Simulations. *J. Atmos. Sci.*, 69, 969–987.
- Levin, Z., Ganor, E., Gladstein, V., 1996. The effects of desert particles coated with sulfate on rain formation in the eastern mediterranean. *J. App. Meteor.*, 35, 1511-1523.
- Mesinger, F., et al., 2006. North American regional reanalysis. *Bull. Am. Meteorol. Soc.*, 87, 343–360.
- Neff, J. C., Reynolds, R. L., Belnap, J., Lamothe, P., 2005. Multi-decadal impacts of grazing on soil physical and biogeochemical properties in southeast Utah. *Ecol. Appl.* 15, 87–95.
- Neff, J. C., Ballantyne, A. P., Farmer, G. L., Mahowald, N. M., Conroy, J. L., Landry, C. C., Overpeck, J. T., Painter, T. H., Lawrence, C. R., Reynolds, R. L., 2008. Increasing eolian dust deposition in the western United States linked to human activity. *Nat. Geosci.*, 1, 189–195, doi:10.1038/ngeo133.
- Niemand, M., Moehler, O., Vogel, B., Vogel, H., Hoose, C., Connolly, P., Klein, H., Bingemer, H., DeMott, P., Skrotzki, J., Leisner, T., 2012. Parameterization of immersion freezing on mineral dust particles: an application in a regional scale model. *J. Atmos. Sci.*, 69, 3077–3092.
- Orgill. M. M., Sehmel, G. A., 1976. Frequency and diurnal variation of dust storms in the contiguous USA. *Atmos. Environ.* 10, 813-825.
- Park, R. J., Jacob, D. J., Field, B. D., Yantosca, R. M., 2004, Natural and transboundary pollution influences on sulphate-nitrate- ammonium aerosols in the United States: Implications for policy. *J. Geophys. Res.*, 109, D15204.
- Park, R. J., Jacob, D. J., Naresh, K., Yantosca, R. M., 2006, Regional visibility statistics in the United States: Natural and transboundary pollution influences and implications for the Regional Haze Rule. *Atmos. Environ.*, 40, 5405–5423.
- Park, R. J., Jacob, D. J., Chin, M., Martin, R. V., 2003. Sources of carbonaceous aerosols over the United States and implications for natural visibility. *J. Geophys. Res.*, 108(D12), D15204.

- Park, S. H., et al., 2007. Simulation of entrainment and transport of dust particles within North America in April 2001 - red dust episode. *J. Geophys. Res.*, 112.
- Painter, T. H., Barrett, A. P., Landry, C. C., Neff, J. C., Cassidy, M. P., Lawrence, C. R., McBride, K. E., Farmer, G. L., 2007. Impact of disturbed desert soils on duration of mountain snow cover. *Geophys. Res. Lett.*, 34, L12502, doi:10.1029/2007GL030284.
- Painter, T. H., Deems, J., Belnap, J., Hamlet, A., Landry, C. C., Udall, B., 2010. Response of Colorado River runoff to dust radiative forcing in snow. *P. Natl. Acad. Sci.*, published ahead of print September 20, 2010.
- Reynolds, C., Cropmton, L., Mills, J., 2010. Livestock and climate change impacts in the developing world. *Outlook Agric.* 39, 245-248.
- Roberts, P., Hallett, J., 1968. A Laboratory Study Of Ice Nucleating Properties Of Some Mineral Particulates. *Quarterly Journal Of The Royal Meteorological Society*, 94(399), 25.
- Sassen, K., Demott, P., Prospero, J., Poellot, M., 2003. Saharan dust storms and indirect aerosol effects on clouds: Crystal-face results. *Geophys. Res. Lett.*, 30, 12, 1633.
- Schaefer, M. B., 1954. Some aspects of the dynamics of populations, important for the management of the commercial marine fisheries. *Inter-Am. Trop. Tuna Comm. Bull.*, 1:27-56.
- Schaefer, V. J., 1949. The formation of ice crystals in the laboratory and the atmosphere. *Chem. Rev.*, 44, 291-320.
- Skiles, S. M., Painter, T. H., Deems, J. S., Bryant, A. C., Landry, C. C., 2012. Dust radiative forcing in snow of the Upper Colorado River Basin: Part II. Interannual variability in radiative forcing and snowmelt rates. *Water Resour. Res.*, 48, W07522.
- Saleeby, S. M., Cotton, W. R., Lowenthal, D., Borys, R. D., Wetzal, M. A., 2009. Influence of cloud condensation nuclei on orographic snowfall. *J. Appl. Meteor. & Clim.*, 48, 903-922.
- Saleeby, S. M., Cotton, W. R., Lowenthal, D., 2011. Impact of aerosols on the microphysical processes with an orographic cloud environment. 2011 AMS Annual Meeting, Seattle, WA.
- Tanaka, T. Y., Chiba, M., 2006. A numerical study of the contributions of dust source regions to the global dust budget. *Glob. Planet. Change* 52, 88–104.
- Tripoli, G., 2006. Local Mesoscale Circulation Systems. Lecture held on April 6, 2006, at the University of Wisconsin, Madison. Retrieved February 3, 2014 from http://mocha.aos.wisc.edu/453_spr06/lecture_06.ppt.
- Tobo, Y., Prenni, A. J., DeMott, P. J., Huffman, J. A., McCluskey, C. S., Tian, G., Pöhlker, C., Pöschl, U., Kreidenweis, S. M., 2013. Biological aerosol particles as a key determinant of ice nuclei populations in a forest ecosystem, *J. Geophys. Res. Atmos.*, 118, 10100–10110.

Uematsu, M., Duce, R., Prospero, J., Chen, L., Merrill, J., McDonald, R., 1983. Transport of mineral aerosol from Asia over the North Pacific Ocean. *J. Geophys. Res.*, 88, 5343–5352.

van den Heever, S. C., Carrio, G. G., Cotton, W. R., DeMott, P. J., 2006. Impacts of nucleating aerosol on Florida storms. Part I: Mesoscale simulations. *J. Atmos. Sci.*, 63, 1752-1775.

Ward, D. S., Cotton, W. R., 2010. Cold and transition season cloud condensation nuclei measurements in western Colorado. *Atmos. Chem. Phys. Discuss.* 10, C11358–C11361.

Ward, D.S., Eidhammer, T., Cotton, W. R., Kreidenweis, S. M., 2010. The role of the particle size distribution in assessing aerosol composition effects on simulated droplet activation. *Atmos. Chem. Phys.*, 10, 5435–5447.

Yin, Y., et al., 2002. Interactions of mineral dust particles and clouds: Effects on precipitation and cloud optical properties. *J. Geophys. Res.*, 107, 4724.

Zuberi, B., Bertram, A., Cassa, C., Molina, L., Molina, M., 2002. Heterogeneous nucleation of ice in $(\text{NH}_4)_2\text{SO}_4\text{-H}_2\text{O}$ particles with mineral dust immersions. *Geophys. Res. Lett.*, 29, 1504.

CHAPTER 4

Summary and Future Work

4.1.1 Overall Summary

The main conclusions from the results of Part I and Part II are as follows:

- The results of the season-long simulations are very sensitive to the details of the microphysics models. Relatively modest variations in CCN activation schemes and IN activation schemes can lead to almost no net affect of aerosol pollution and dust on winter-season total precipitation or substantial precipitation losses.

Using our best estimates of IN nucleation scheme and dust acting as CCN we find that the combined affects of anthropogenic pollution and dust can lead to 2.32 % or 6,070,000 acre-ft losses in precipitation over our fine grid domain, and a decrease 1.9 % or 4,020,000 acre-ft for the CRB for a period of almost ~6.5 months when dust is not in the clean background run. When dust is included in the clean run, it was found that the net change in domain total integral winter-season precipitation using Setup 3 was a reduction of 2.56 % for the Grid 3 and a decrease in 2.1 % for the CRB compared to the run with no anthropogenic aerosol sources. This corresponds to total winter-season precipitation loss due to anthropogenic pollution of 5,380,00 acre-feet of water for the ~ 6.5 months of simulation for the CRB. This is an appreciable amount of water and represents around 72 % of total water allocated under the CRB compact.

- Sensitivity studies suggest that the impact of dust in a system is largely dependent on the synoptic scale flow and the amount of moisture available for a particular case study. Increasing amounts of dust has a larger impact on wet weather systems.
- In Case Study 1, a wet system, dust increases precipitation in the CRB by 0.49% when increased 3 times and 1.29 % when dust is increased 10 times. So, in Case 1, the cloud base heights are higher than Case Study 3 and lower than Case Study 2, and adding dust as IN increased precipitation. The dust IN effects are dominant and there is more precipitation when dust acts only as IN. But the increase is not huge.
- In Case Study 2, dust decreases precipitation in the CRB by -4.63% when increased 3 times and -5.62% when dust is increased 10 times. This system has less precipitable water and other meteorological factors like high southwesterly wind flow favors enhanced blow-over and over-seeding the clouds.
- In Case 3, cloud bases are lower, so the base temperatures are warmer, an active drizzle formation process is present, and dust CCN effects are more dominant. So we see non-monotonicity in response and suppression of drizzle formation, which is similar to the results of Carrio and Cotton (2014).

4.2.1 Future Work

It would be useful to run the same simulations with the updated code and examine the cumulative effect of dust acting as CCN, GCCN, and IN over the entire Colorado Rocky Mountains for the snow years 2004-2005, 2005-2006, 2006-2007 and 2007-2008. Another long term goal could be the use of the Variable Infiltration Capacity model (Painter et al., 2010) to predict the combined effects of dust on snowpack and dust acting as cloud-nucleating aerosol on water resources in the CRB. However, it is important to consider the effects of earlier runoff on

total water loss by evaporation and melting of snowpack with a large surface area relative to evaporation loss in reservoirs which have reduced surface areas. This would give us further insight on the total hydrological impacts of anthropogenic aerosol and dust.

REFERENCES

McCabe, G. J., Wolock, D. M., 2007. Warming may create substantial water supply shortages in the Colorado River basin. *Geophysical Research Letters* 34: doi: 10.1029/2007GL031764. issn: 0094-8276.

APPENDIX

Table A.1: Table for the basin wise difference in precipitation in the CRB

AREA	RIVER BASIN	CLEAN	DIRTY	DIF
1	Alamosa Trinchera	7.19E+12	7.01E+12	-2.52
2	Animas	7.33E+12	7.31E+12	-0.26
3	Apishapa	1.80E+12	1.73E+12	-4.06
4	Arkansas Headwaters	1.17E+13	1.15E+13	-2.12
5	Big Sandy	2.69E+11	2.59E+11	-4.00
6	Big Thompson	2.74E+12	2.71E+12	-0.85
7	Bijou	1.63E+12	1.56E+12	-4.42
8	Bitter	0	0	0.00
9	Blue	3.66E+12	3.61E+12	-1.52
10	Cache La Poudre	2.89E+12	2.81E+12	-2.75
11	Canadian Headwaters	4.10E+11	3.91E+11	-4.84
12	Chico	7.19E+11	6.72E+11	-6.53
13	Cimarron	7.10E+09	7.06E+09	-0.61
14	Clear	2.40E+12	2.38E+12	-0.82
15	Colorado Headwaters	1.47E+13	1.43E+13	-2.35
16	Colorado Headwaters Plateau	1.21E+13	1.17E+13	-3.09
17	Conejos	2.87E+12	2.84E+12	0.97
18	Crow	4.14E+11	3.84E+11	-7.38
19	Eagle	5.12E+12	5.02E+12	-1.99
20	East Taylor	4.79E+12	4.69E+12	-1.94
21	Fountain	4.92E+11	4.64E+11	-5.80
22	Horse	5.50E+12	5.45E+12	-0.92
23	Huerfano	3.35E+12	3.28E+12	-2.21
24	Kiowa	2.08E+11	1.93E+11	-6.94
25	Little Snake	1.73E+12	1.72E+12	0.49
26	Lone Tree Owl	7.22E+10	7.11E+10	-1.56
27	Lower Dolores	7.18E+12	7.04E+12	-2.07
28	Lower Green Diamond	0	0	0.00
29	Lower Gunnison	6.02E+10	5.89E+10	-2.28
30	Lower Lodgepole	2.28E+12	2.22E+12	-2.90
31	Lower San Juan/Four Corners	3.36E+12	3.25E+12	-3.39
32	Lower White	2.59E+12	2.58E+12	0.39
33	Lower Yampa	1.48E+12	1.49E+12	0.13
34	Mancos	2.06E+12	2.04E+12	0.93
35	Mcelmo	3.18E+12	3.00E+12	-5.64

36	Middle San Juan	1.84E+11	1.70E+11	-7.70
37	Middle South Platte/Cherry Creek	3.93E+11	3.93E+11	0.11
38	Middle South Platte–Sterling	0	0	0.00
39	Montezuma	5.29E+12	5.09E+12	-3.74
40	Muddy	6.99E+12	6.85E+12	-1.93
41	North Platte Headwaters	3.13E+12	3.07E+12	-1.85
42	North Fork Gunnison	1.91E+11	1.72E+11	-9.51
43	Parachute Roan	1.87E+12	1.79E+12	-4.37
44	Pawnee	4.00E+12	3.82E+12	-4.39
45	Piceance Yellow	5.63E+12	5.56E+12	-1.30
46	Piedra	9.42E+12	9.21E+12	-2.20
47	Purgatorie	1.22E+11	1.16E+11	-5.35
48	Rio Chama	3.51E+12	3.34E+12	-4.73
49	Rio Grand Headwaters	5.05E+12	4.98E+12	-1.42
50	Roaring Fork	7.30E+12	7.25E+12	0.79
51	Rush	3.73E+12	3.64E+12	-2.30
52	Saguache	4.30E+12	4.24E+12	-1.25
53	San Luis	4.12E+12	4.05E+12	-1.84
54	San Miguel	5.06E+12	4.97E+12	-1.79
55	Sidney Draw	6.95E+12	6.81E+12	-2.07
56	South Platte Headwater	1.25E+12	1.17E+12	-6.12
57	St. Vrain	8.24E+12	8.34E+12	1.20
58	Tomichi	3.50E+11	3.37E+11	-3.80
59	Uncompahange	1.08E+13	1.06E+13	-2.29
60	Upper Arkansas	1.31E+12	1.29E+12	-1.92
61	Upper Arkansas/Lake Meredith	1.67E+09	1.56E+09	-6.61
62	Upper Dolores	3.82E+11	3.76E+11	-1.41
63	Upper Green/Flaming Gorge Res	2.07E+11	1.83E+11	-11.32
64	Upper Gunnison	1.10E+13	1.11E+13	0.44
65	Upper Laramie	6.06E+12	5.96E+12	-1.70
66	Upper Lodgepole	6.14E+12	6.04E+12	-1.68
67	Upper North Platte	1.27E+13	1.25E+13	-1.59
68	Upper Rio Grande	4.09E+11	3.92E+11	-4.19
69	Upper San Juan	5.30E+11	5.14E+11	-3.01
70	Upper South Platte	2.16E+12	2.13E+12	-1.32
71	Upper White	9.19E+11	8.92E+11	-2.93
72	Upper Yampa	3.95E+12	3.95E+12	0.14
73	Vermilion	1.00E+12	1.02E+12	1.49
74	Westwater Canyon	1.85E+10	1.70E+10	-7.82